

Critical review of elemental composition measurements in the PeV range

G. Di Sciascio

*INFN - Roma Tor Vergata, Italy
disciascio@roma2.infn.it*

The 2nd LHAASO SYMPOSIUM **21-24 MARCH 2025
HONG KONG, CHINA**



Introduction

Cosmic Rays above about 100 TeV/n can be studied in a statistically significant way only from ground operating detectors (arrays/telescopes)

The reconstruction of the primary characteristics (energy, mass, arrival direction) is carried out in an indirect way exploiting the detection of Extensive Air Showers.

Strictly speaking, *no air shower experiment measures the primary composition of CRs.*

We exploit different EAS observables *statistically related* to the mass of the primary CR

But the sensitivity to the mass of these observables are different, even because they investigate *different kinematic regions* of the hadronic interaction undergone by the primary particle.

According to the results obtained by a number of experiments in the last decades I will show you that *the reconstructed primary spectra of the different components seems to depend on the explored kinematic region.*

Measurement of the elemental composition

What is the meaning of measuring the elemental composition?

Selection of different primary nuclei event-by-event, according to some criteria

On average there is a correlation between some observables and cosmic-ray mass, although mass determination of single events is challenging due to *intrinsic mass-separation limits* (shower-to-shower fluctuations) for the individual observables.

The measured observables were compared with a simulated ensemble of events, *on statistical basis only*. The simulations were done with several interaction models and composition spectra.

These studies determine the *probability of triggering the experiment as a function of mass and energy*.

This challenge can be alleviated by combining knowledge of multiple mass sensitive observables, which yields the best prospects for cosmic-ray mass determination

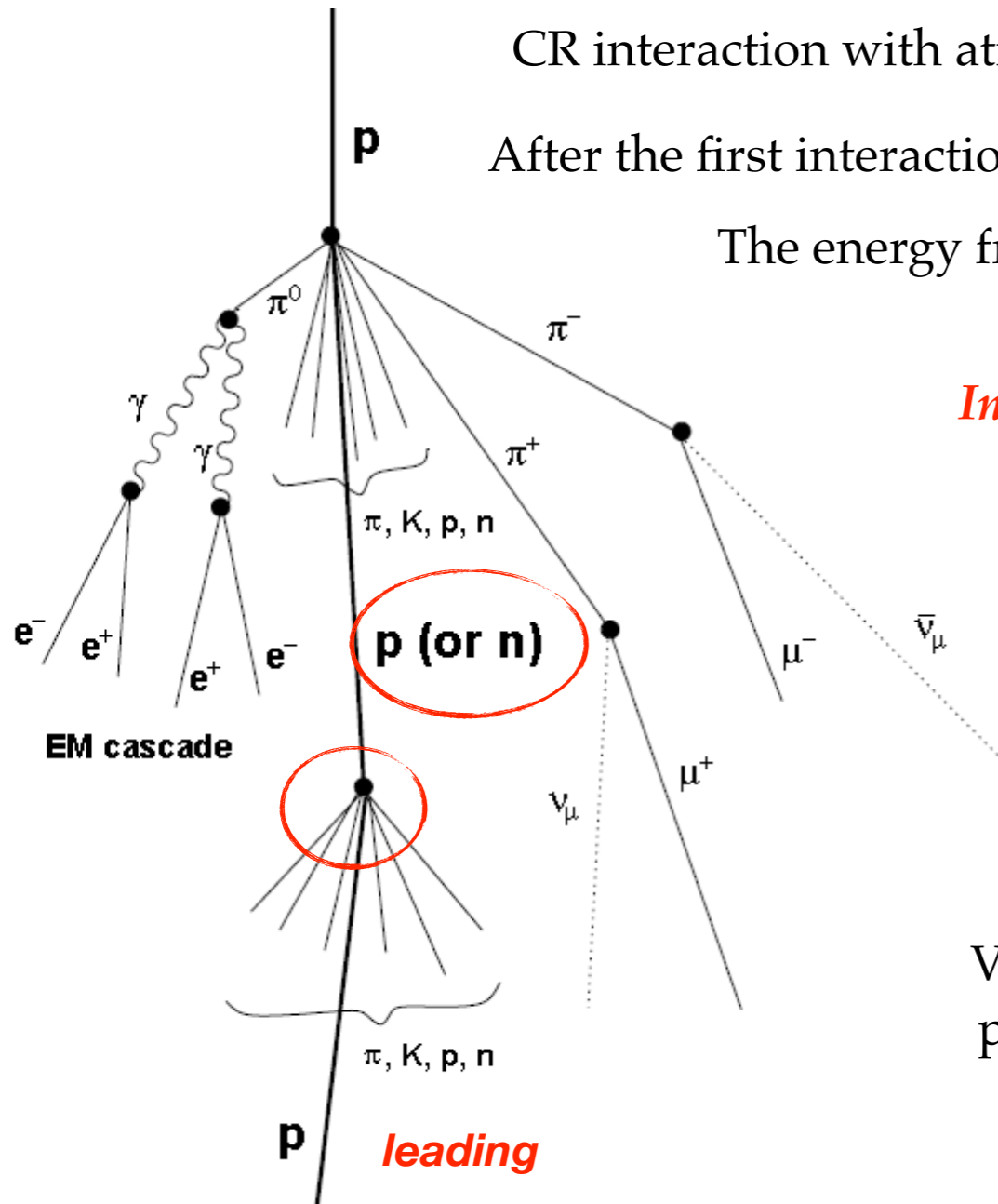
Measurement of the elemental composition

In principle, for better estimation of the CR composition, *observation of air shower development at its early stage*, close to the first interaction, which strongly reflects the atomic mass number of the primary CR, is the most suitable way.

To reduce the systematic uncertainties and to unveil the details of the spectrum we need:

- Measure EAS near *maximum development depths* to reduce EAS fluctuations
- Use an *unbiased trigger threshold* for heavy components because EAS developments are faster than those of light components at a same energy.
- Measure the *electromagnetic components* which are less dependent on hadronic interaction model than the muon component in EASs.
- Require a *enough separation capability* between different species (p, He, CNO, MgSi, Fe ?).
- Measure the chemical composition with *wide energy range* (from direct measurement region to above the knee) for cross calibration.

Hadronic interactions



CR interaction with atmosphere is an hadronic interaction: pN, NN interaction

After the first interaction the *proton propagates deep in atmosphere* with reduced energy.

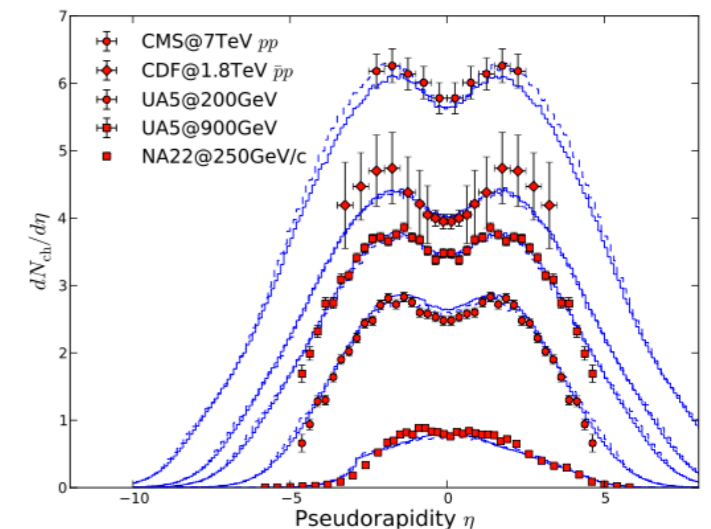
The energy fraction carried by nucleons is the “*elasticity*” of the interaction.

Inelasticity $k = 1 - \frac{E_{lead}}{E_p}$ → *leading energy fraction*

The spectrum of nucleons produced in hadronic interactions plays a fundamental role in the development of EAS.

These high-energy *nucleons feed energy deeper* into the EAS.

Very difficult to measure leading particles in collider experiments



Measurements at colliders are limited to an angular region that excludes the beam pipe, and therefore a very large *majority of the high energy particles that are emitted at small angles are unobservable.*

10 PeV proton with $x_{Lab} = 0.3$ implies a scattering angle of secondary particle of \approx few μ rad

Feynman x and rapidity

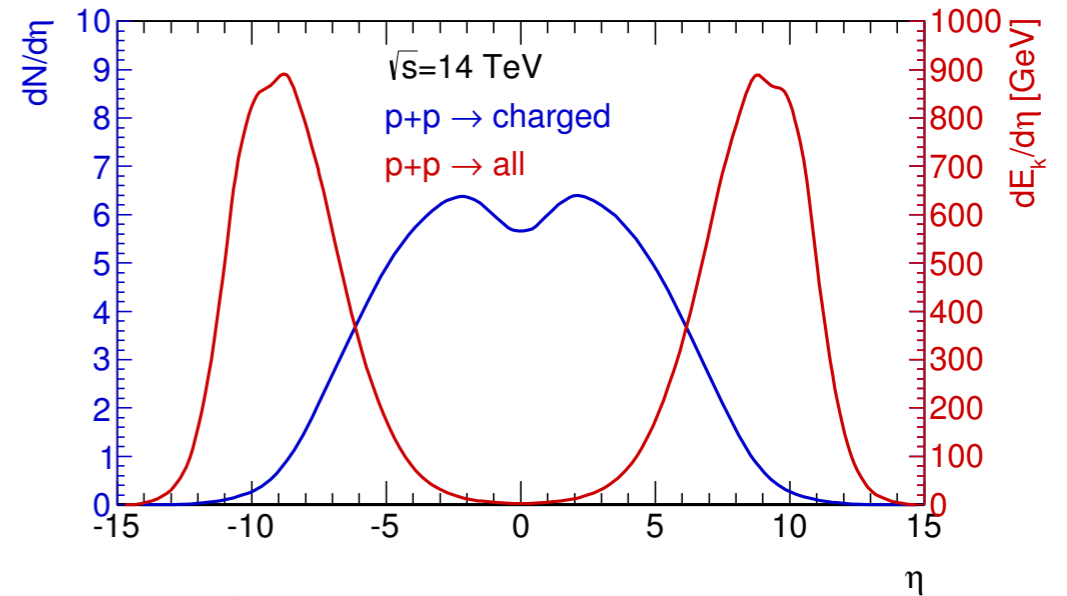
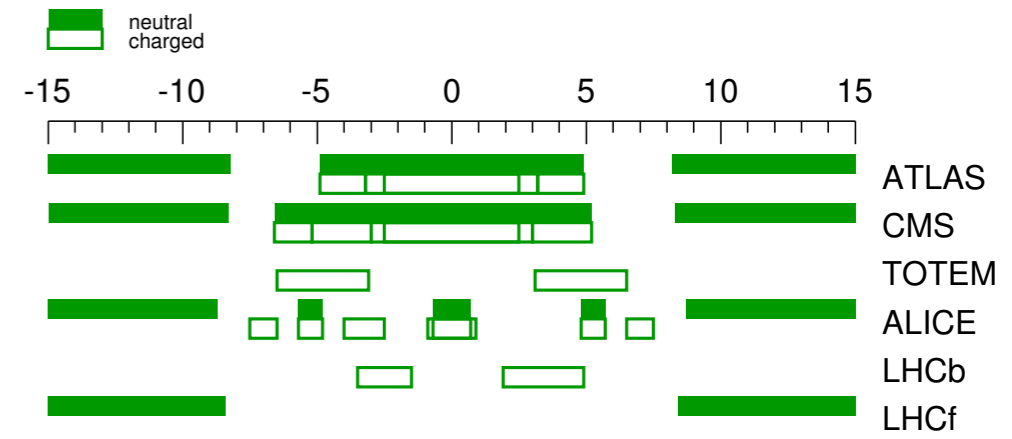
Feynman x: $x_F = \frac{p_z}{p_{max}} \approx 2 \frac{p_z}{\sqrt{s}}$

$x_{lab} = \frac{p_z}{p_{beam}}$

Pseudorapidity: $\eta = -\ln\left(\tan\frac{\theta}{2}\right)$ θ is the angle wrt. to the beam

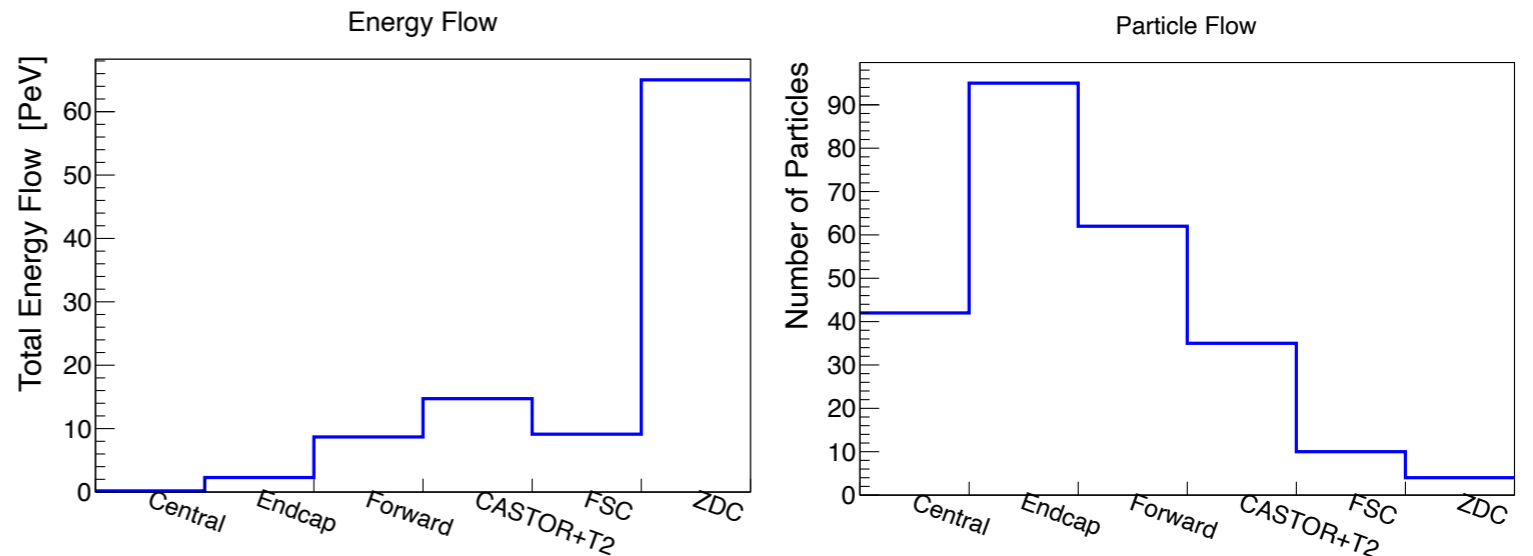
Rapidity: $y = \frac{1}{2} \ln \frac{E + p_z}{E - p_z} = -\ln\left(\tan\frac{\theta}{2}\right) = \eta$ for massless particles

$y_{lab} = y + \frac{1}{2} \ln \frac{1 + \beta}{1 - \beta}$

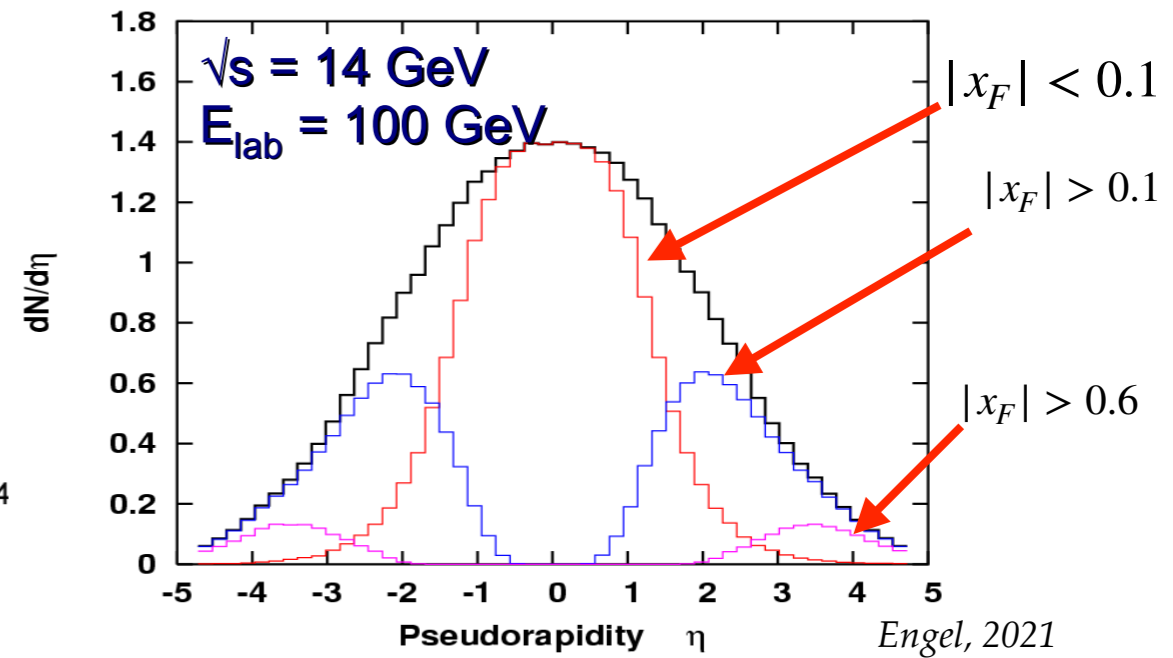
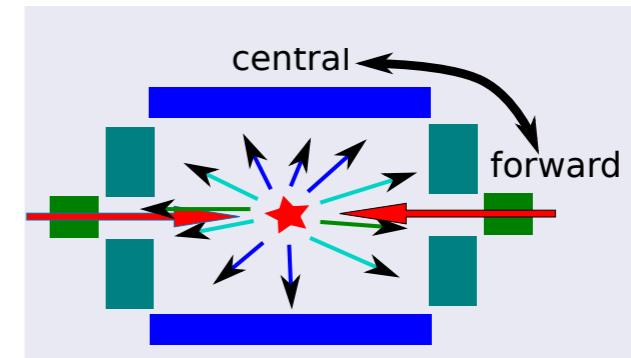
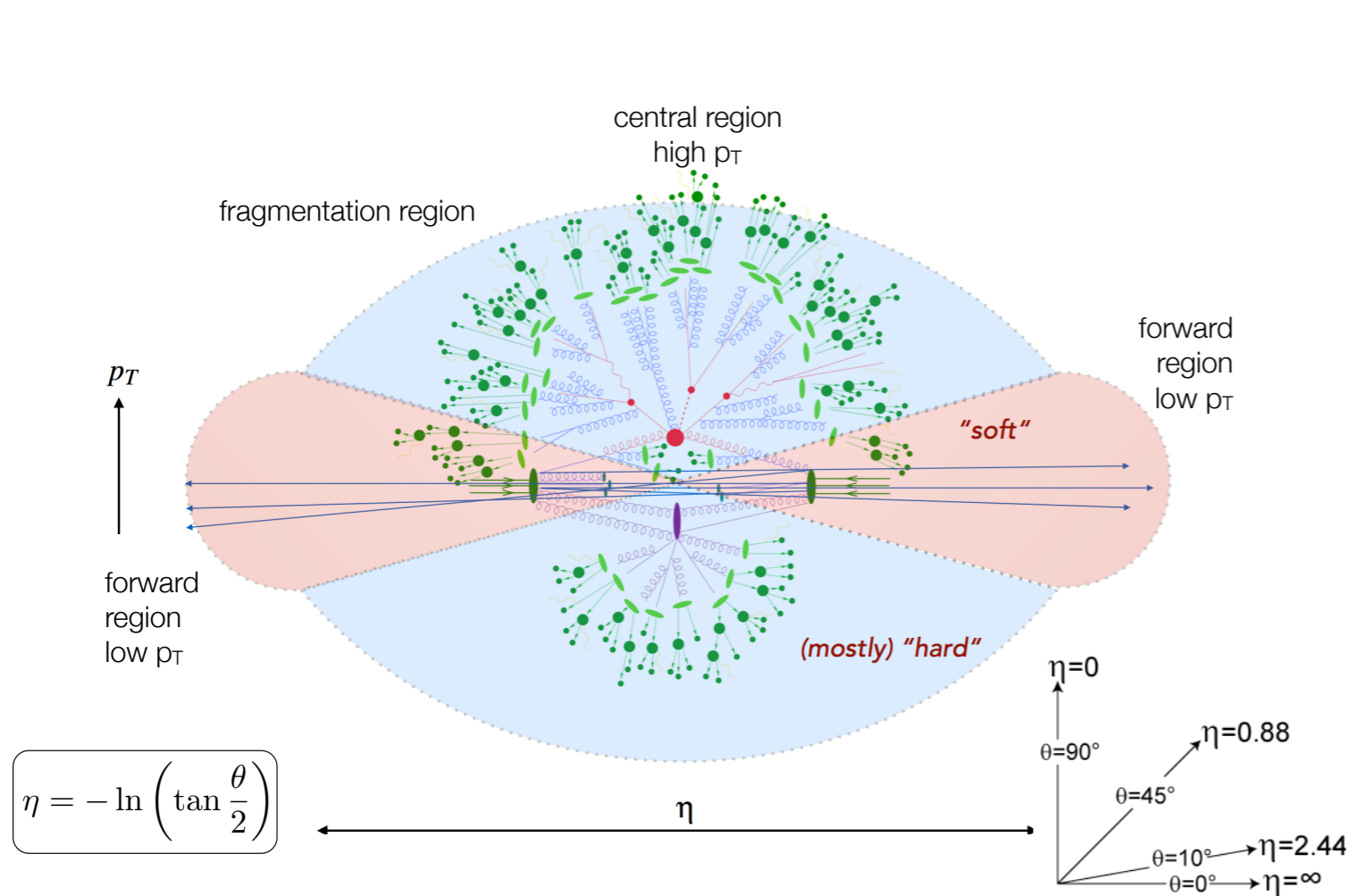


Angular acceptance of LHC experiments

Ulrich, 2021



High energy particle interactions



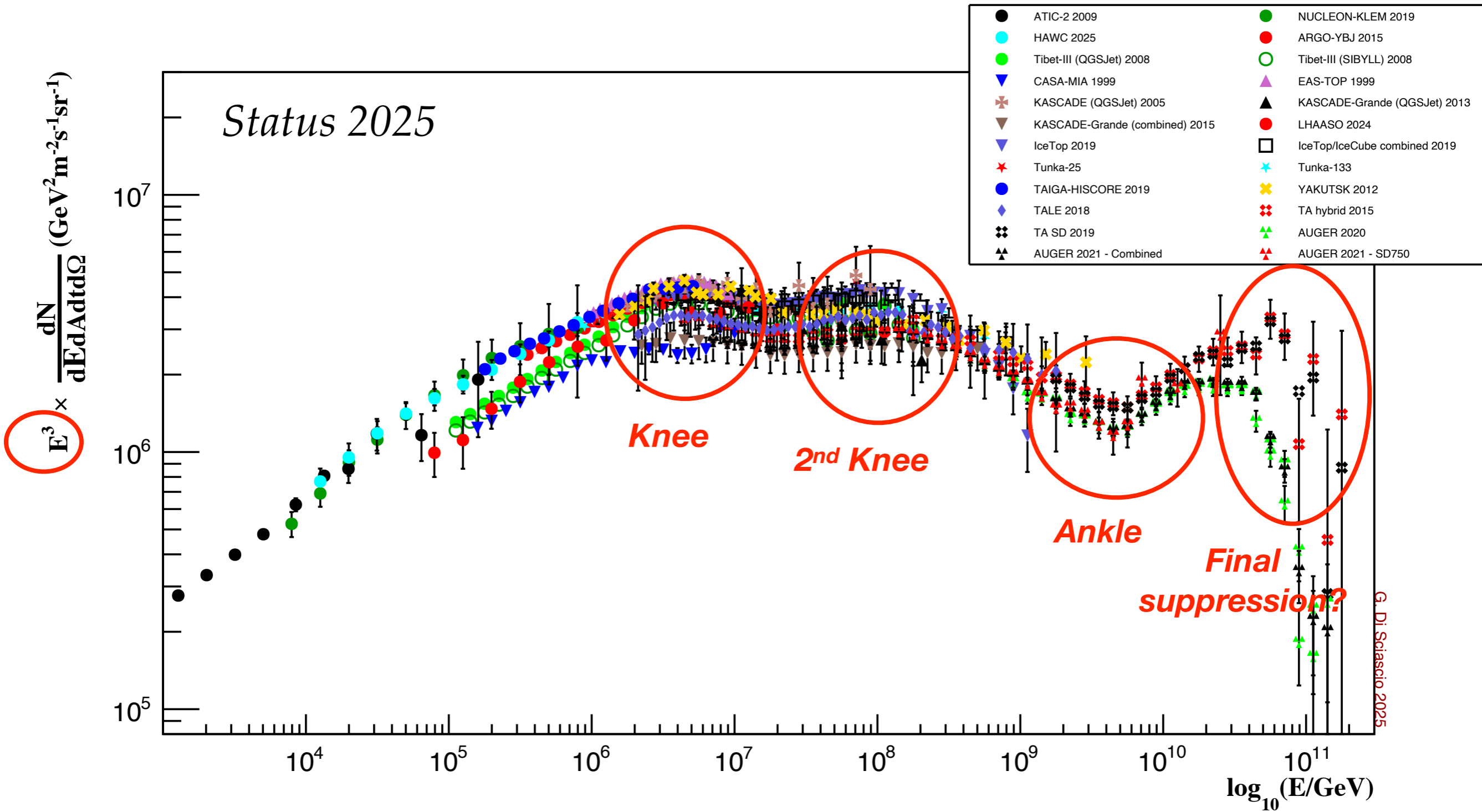
Hard (central) region $|\eta| < 1$

- High particle number density
- Low energy density
- Heavy particles decay in this region
- **Observed by collider experiments**

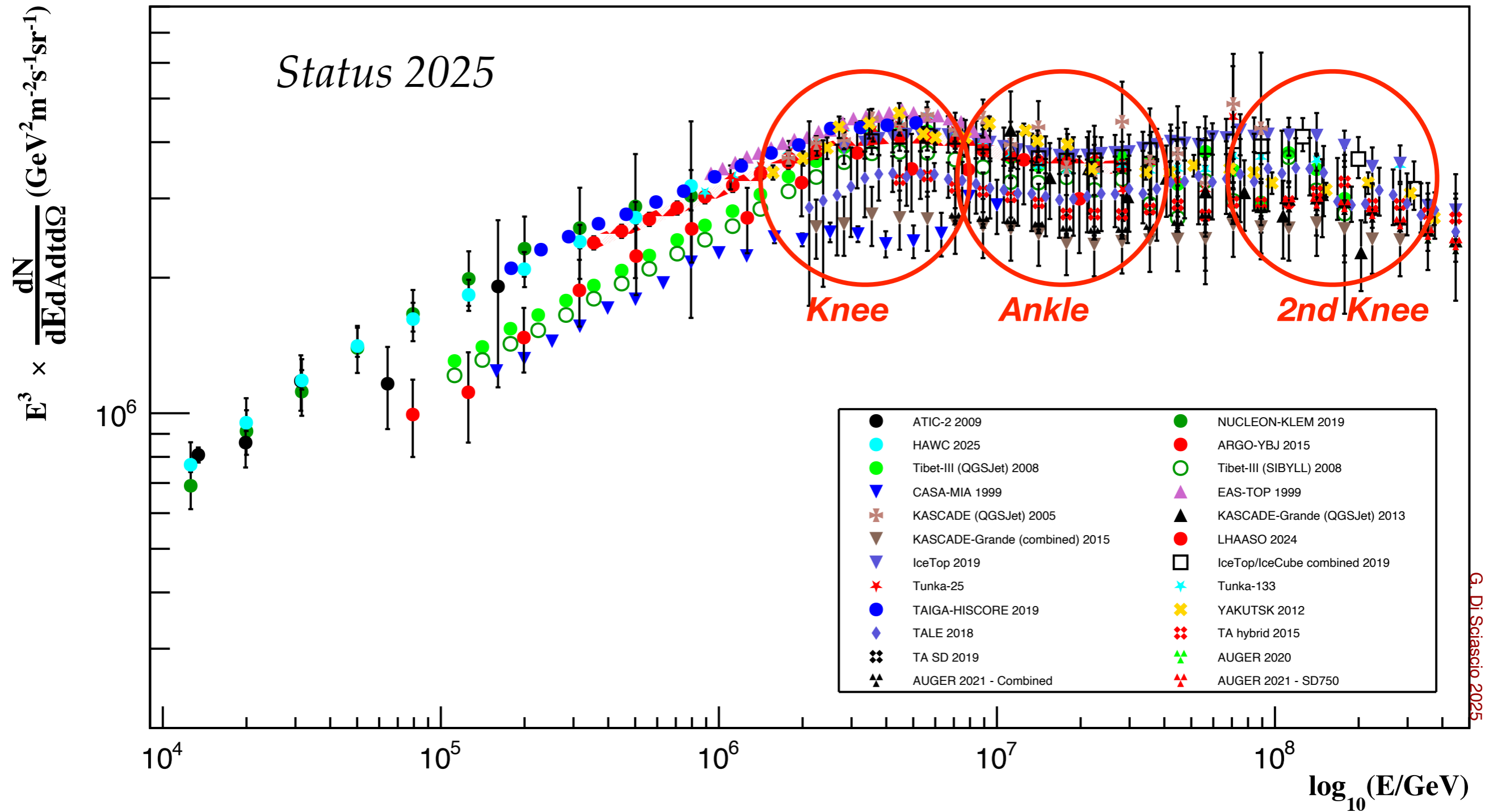
Soft (forward) region $3 < |\eta| < 5$

- Low particle number density
- High energy density
- **Very important in cosmic ray physics**

All-particle Energy Spectrum

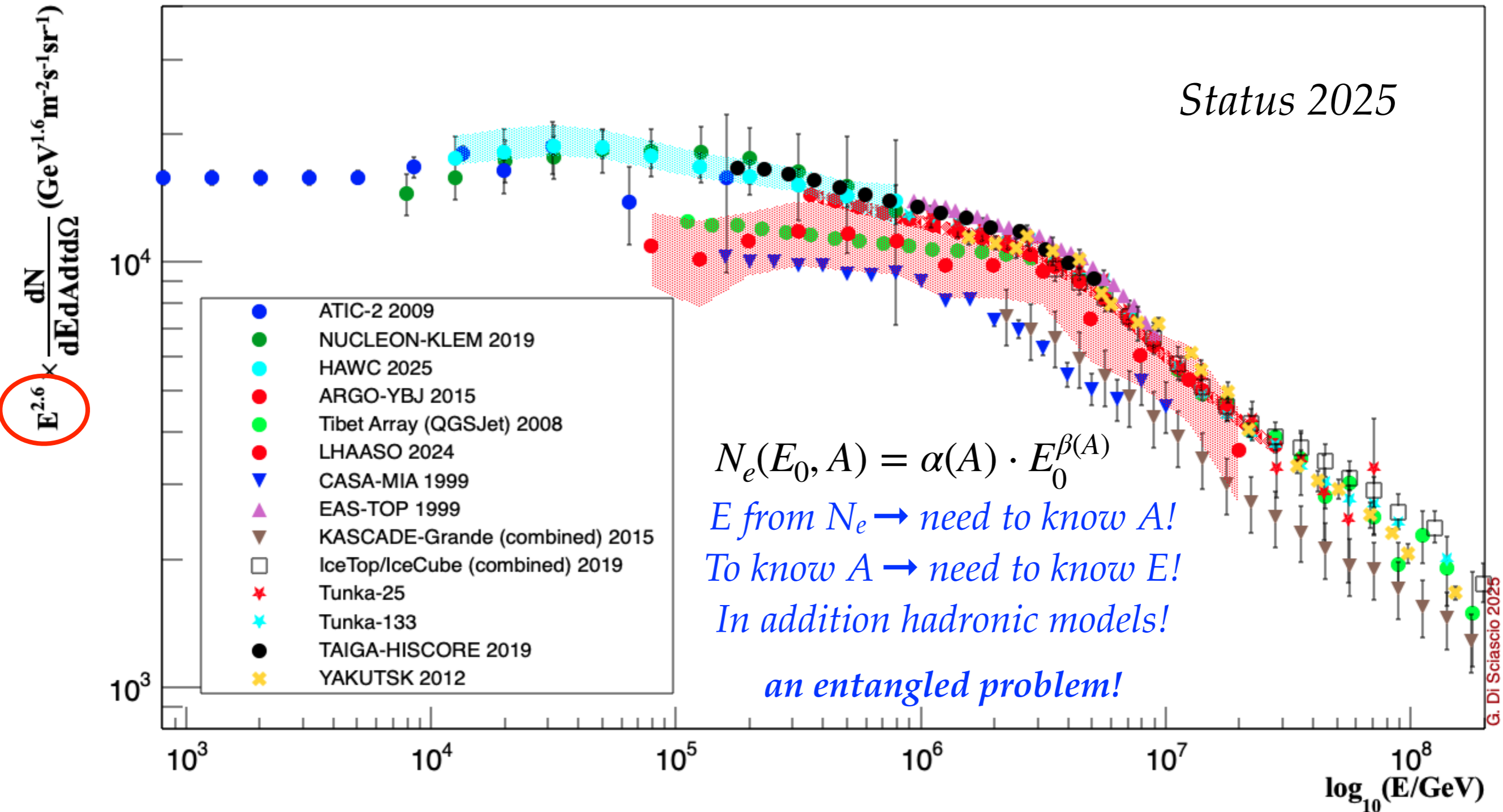


A closer look to the knee region



G. Di Sciascio 2025

A closer look to the knee region



Mass-sensitive EAS observables

We have different mass-sensitive EAS observables

◆ Particle numbers at ground

- electrons
- muons (also underground)
- hadrons

- *the electron-to-muon number ratio*
- *the arrival time distribution*
- *the curvature of the shower front*
- *the slope of the lateral distribution*
- *shower core density*
- *delayed hadrons*
- *underground muons*
- *muon fluctuations*
- ...

$E > 10^{13}$ eV

◆ Cherenkov light

$10^{14} < E < 10^{16}$ eV

◆ Fluorescence light

$E > 10^{17}$ eV

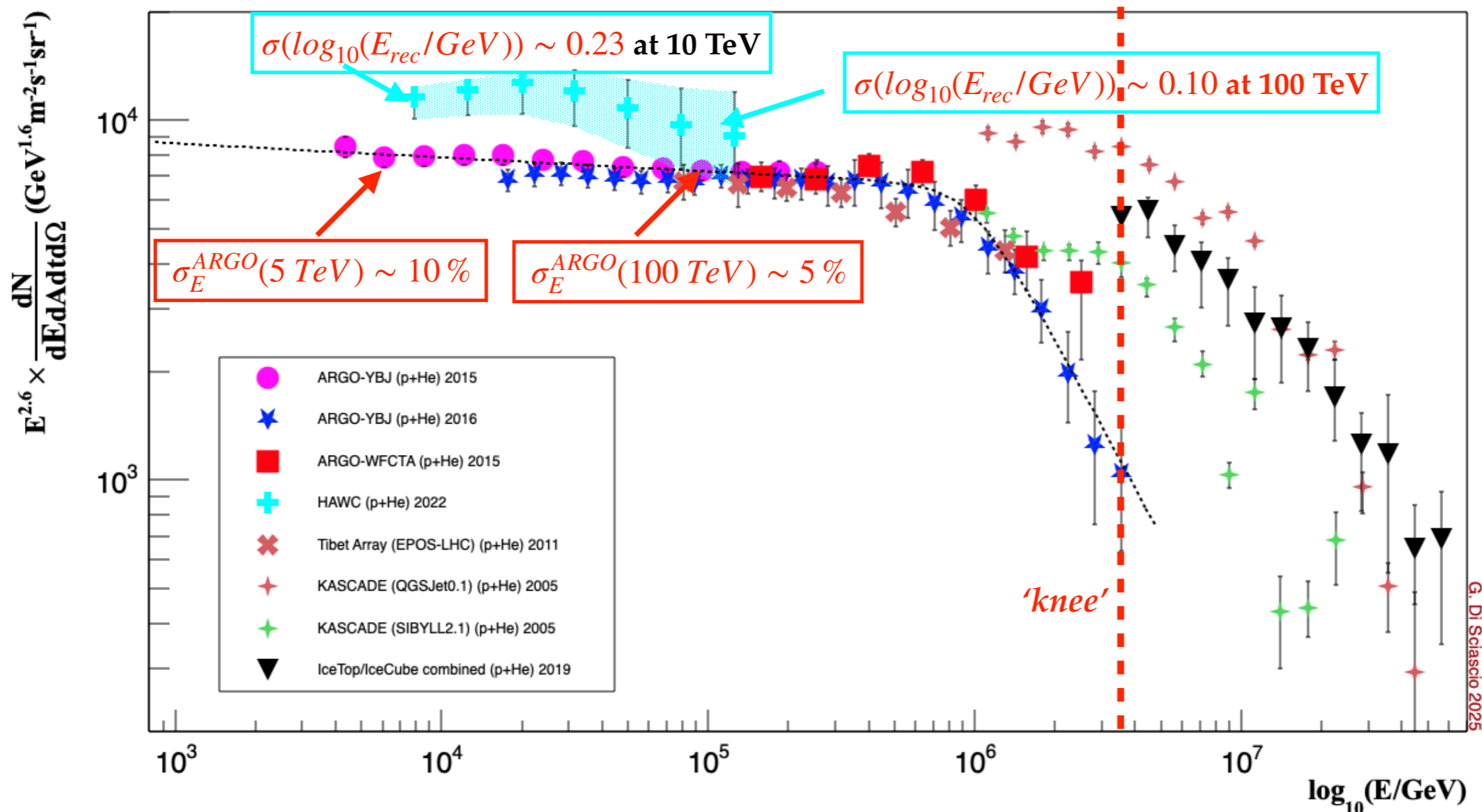
◆ Radio signals

$E > 10^{16}$ eV

$p+He$: indirect measurements

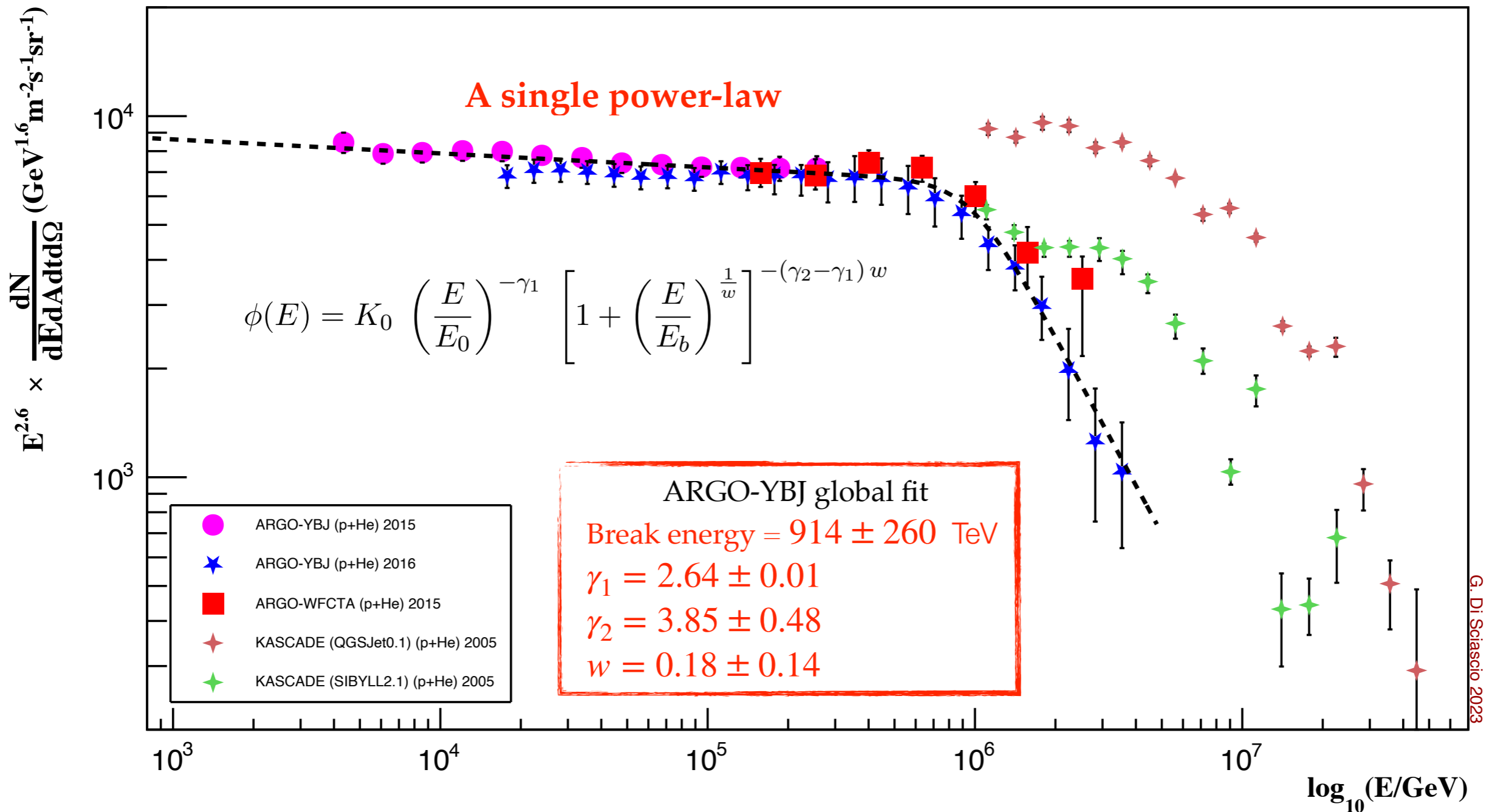
- ✓ **ARGO-YBJ** and **TIBET ASY**: single power law $E < 500$ TeV
- ✓ **HAWC**: deviation from single power law?

- ✓ **ARGO-YBJ** and **TIBET ASY**: light knee below the PeV
- ✓ **KASCADE**: light knee at about 4 PeV



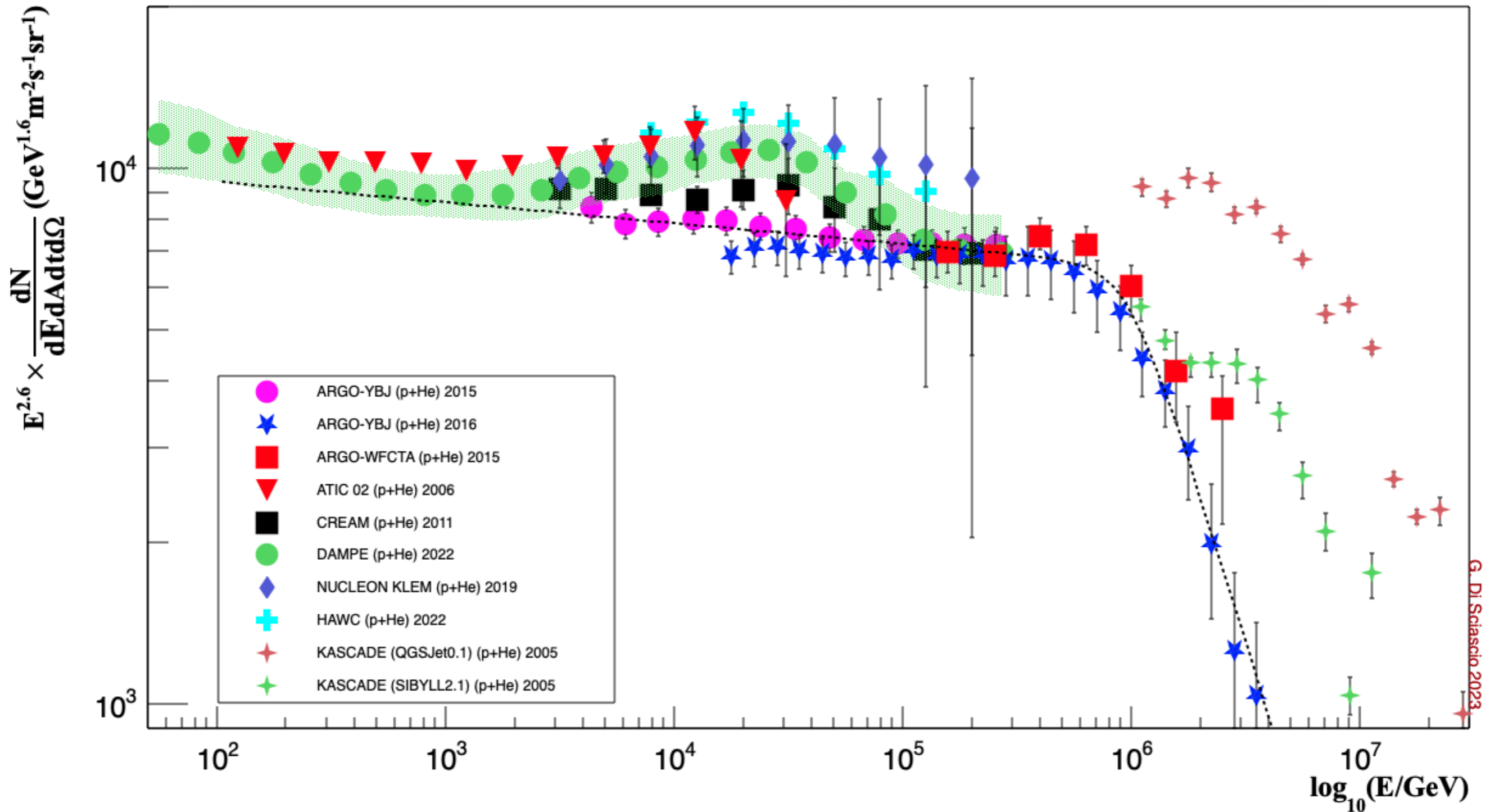
The ARGO-YBJ (p+He) knee

ARGO-YBJ: the only experiment with (p+He) data in the range TeV - 5 PeV
 → clear observation of a knee both with array and a wide FOV Cherenkov Telescope



$p+He$: direct vs indirect measurements

Deviation from a single power-law in the 10 - 100 TeV range?



Why conflicting results?

- Experiments located at different altitudes: sea level → 5200 m asl
- Different detectors and layout
- Different coverage → different sampling capability / fluctuations
- Different energy threshold → calibration absolute energy scale
- Different role of fluctuations which limit mass resolution
- Different energy resolution → better close to the shower max
- Different observables to infer the elemental composition
- *Different kinematic regions explored by the observables*
- Different reconstruction procedures
- ...

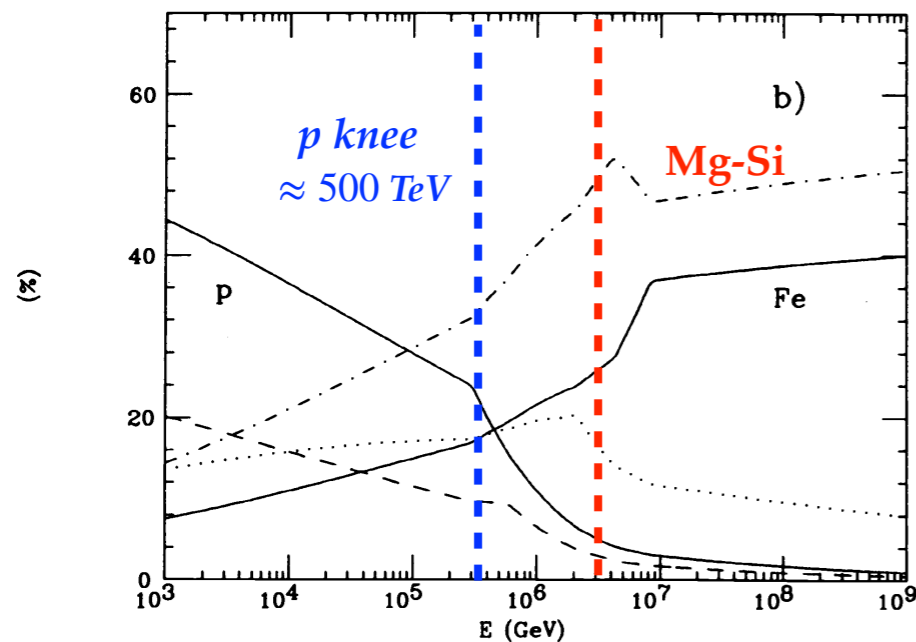
Maryland, 730 and 1000 g/cm²

Pioneering analysis with 2 mass-dependent observables studied *at 2 different altitudes:*

- The temporal spectrum of hadrons with respect to the main front of the shower (*the rate of delayed hadrons near air shower cores*)
- The rate of events which exceed a minimum shower density cut and specific hadronic calorimeter signal cuts

The more penetrating light primary showers are more likely to trigger than are showers from heavy primaries of the same energy.

The trigger and delay rates are sensitive to primary composition because more low-energy *hadron showers from heavy primaries are more likely to produce events with hadrons delayed with respect to the shower front.*



“The data consistent with a *substantial fraction of nuclei heavier than helium at 10¹⁵ eV.*”

VOLUME 42, NUMBER 13

PHYSICAL REVIEW LETTERS

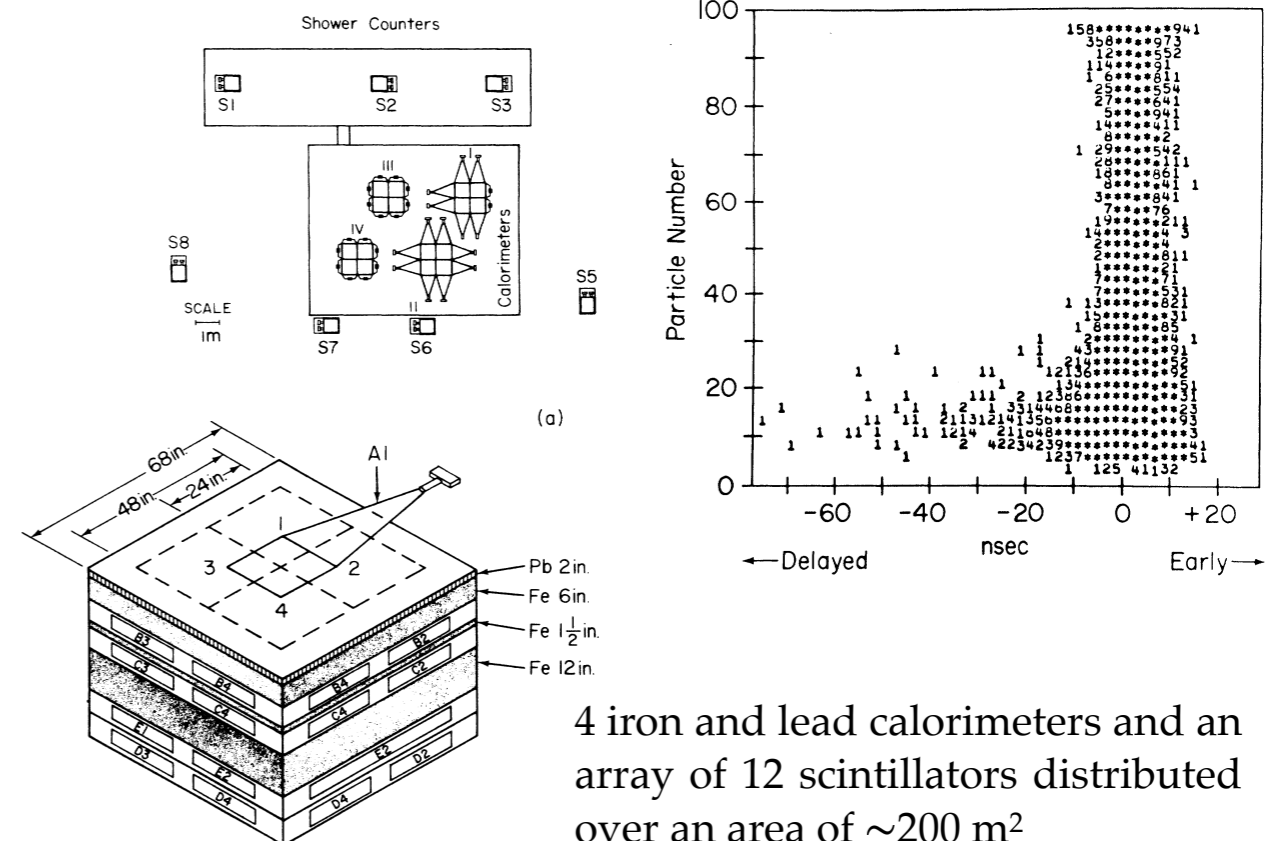
26 MARCH 1979

Composition of Primary Cosmic Rays above 10¹⁵ eV from the Study of Time Distributions of Energetic Hadrons near Air-Shower Cores

J. A. Goodman, R. W. Ellsworth, A. S. Ito,^(a) J. R. MacFall,^(b) F. Siohan,^(c) R. E. Streitmatter, S. C. Tonwar,^(d) P. R. Vishwanath, and G. B. Yodh^(e)

Department of Physics and Astronomy, University of Maryland, College Park, Maryland 20742
(Received 26 December 1978)

An experimental study of the distribution of arrival time of energetic hadrons relative to associated air-shower particles has been made at a mountain altitude, under 730 g cm⁻². Monte Carlo simulations have shown that these observations are sensitive to the composition of primary cosmic rays of energies 10⁴–10⁶ GeV. The energy spectra dN/dE of primary protons and iron-group nuclei required to understand these observations are $1.5 \times 10^4 E^{-2.71 \pm 0.06}$ and $1.27 E^{-2.36 \pm 0.06} \text{ m}^{-2} \text{ sr}^{-1} \text{ sec}^{-1} (\text{GeV}/N)^{-1}$, respectively, where E is the energy per nucleon.

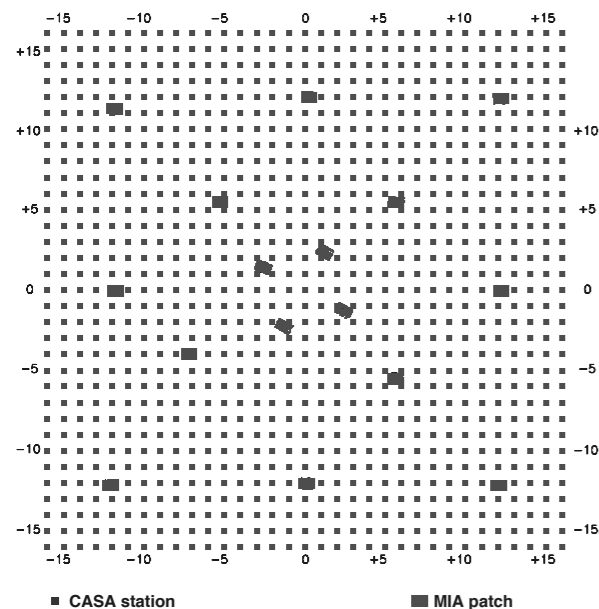


4 iron and lead calorimeters and an array of 12 scintillators distributed over an area of ~200 m²

CASA-MIA, 870 g/cm²

Salt Lake City, Utah 1400 m asl

array of 1089 surface particle detectors (CASA)
and 1024 3 m underground muon detectors (MIA)

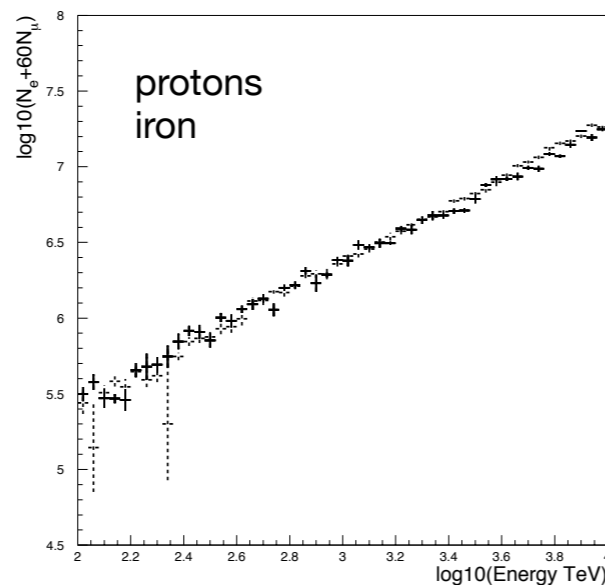
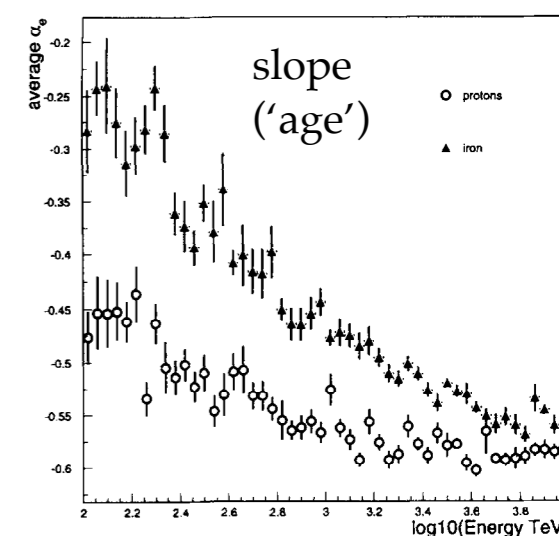
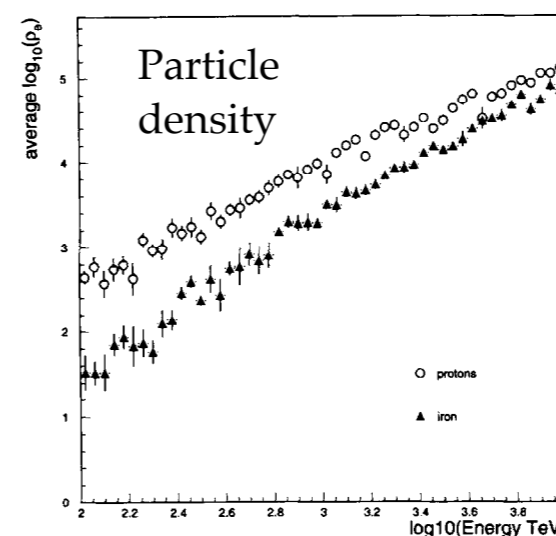


Energy threshold ≈ 100 TeV

Observables in the core are
the most discriminating

Three parameters sensitive to composition

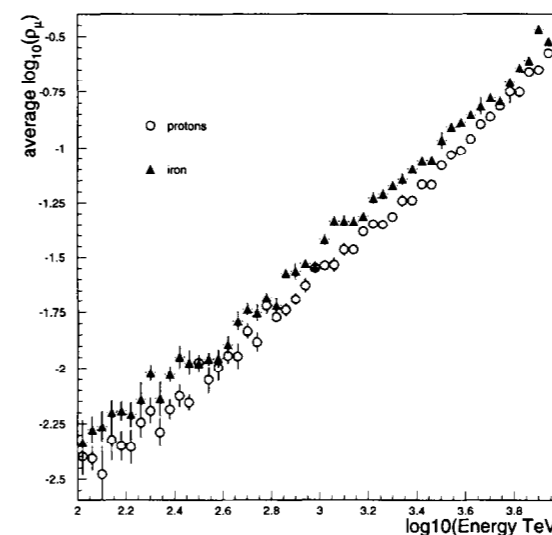
- the density of particles near the core
- the slope of the surface lateral distribution
- the density of muons at large distance (500 m)



$$E_0 \approx A + B \cdot (N_e + K \cdot N_\mu)$$

Mass-independent
energy reconstruction

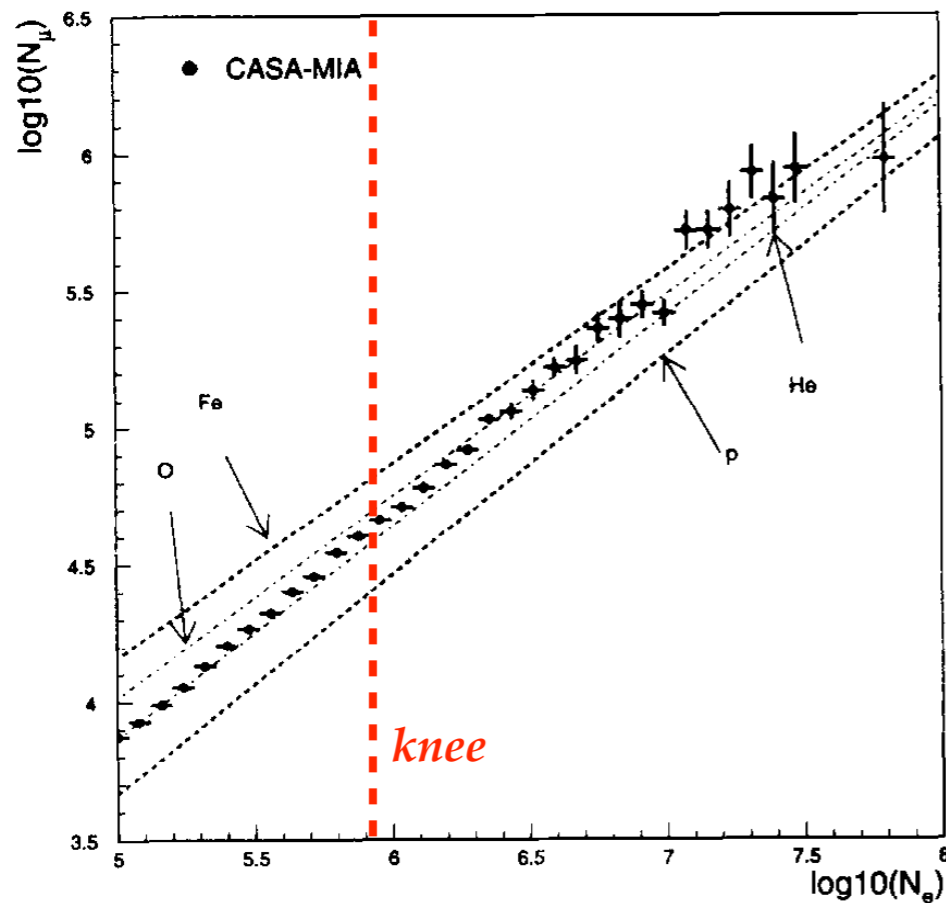
The e.m. lateral distribution function is evaluated near
the core, where proton and iron showers differ the most.



The average muon density
at 500 m from the core

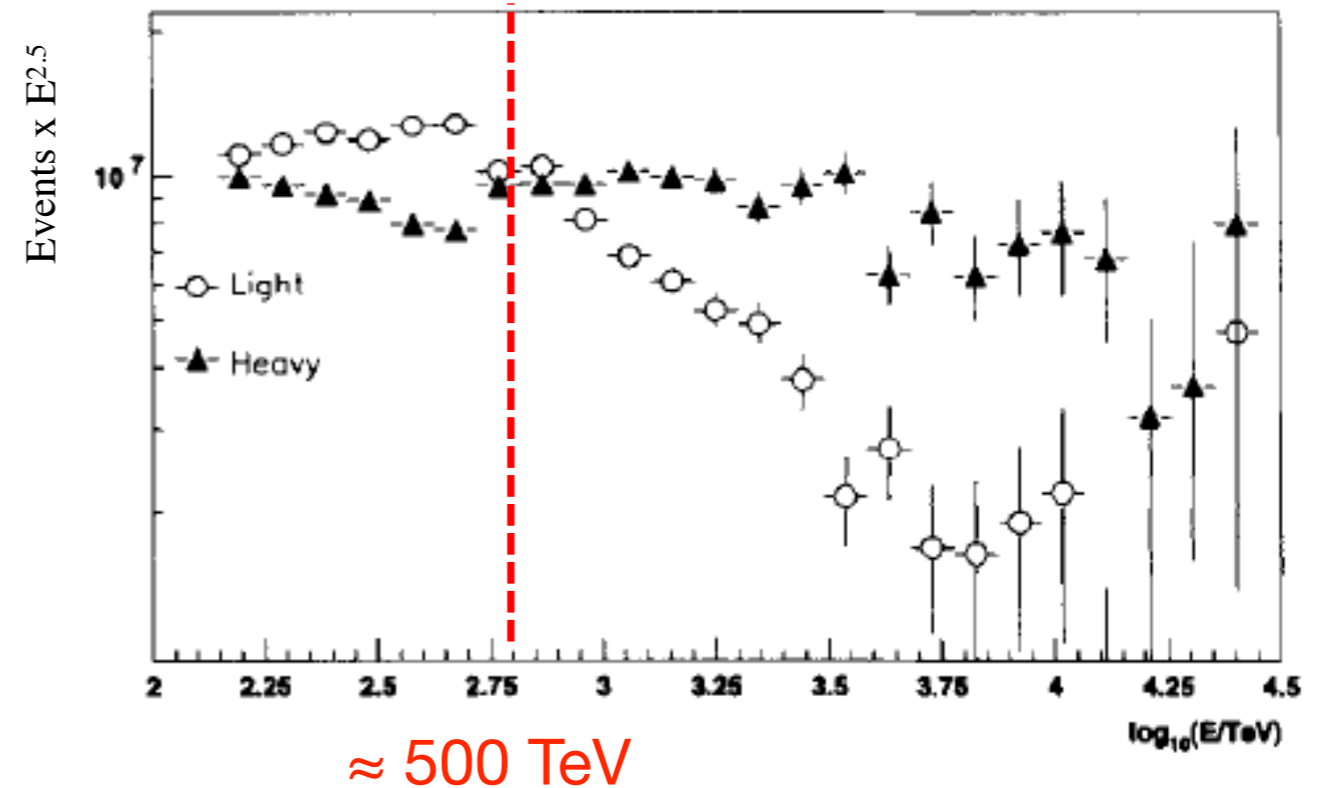
CASA-MIA, 870 g/cm²

Astrop. Phys. 12 (1999) 1-17



Muon size vs electron size

“The shapes of the iron and proton muon lateral distributions are very similar because of the lesser attenuation of the muon component of showers in air”

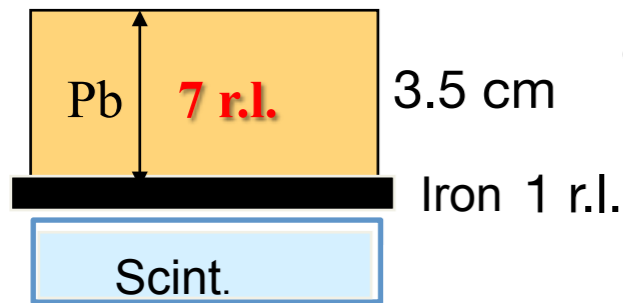


The spectra of the heavy and light components appear similar below 500 TeV, at which point the lighter component's spectral index steepens. The heavier component shows no such “knee” at that energy.

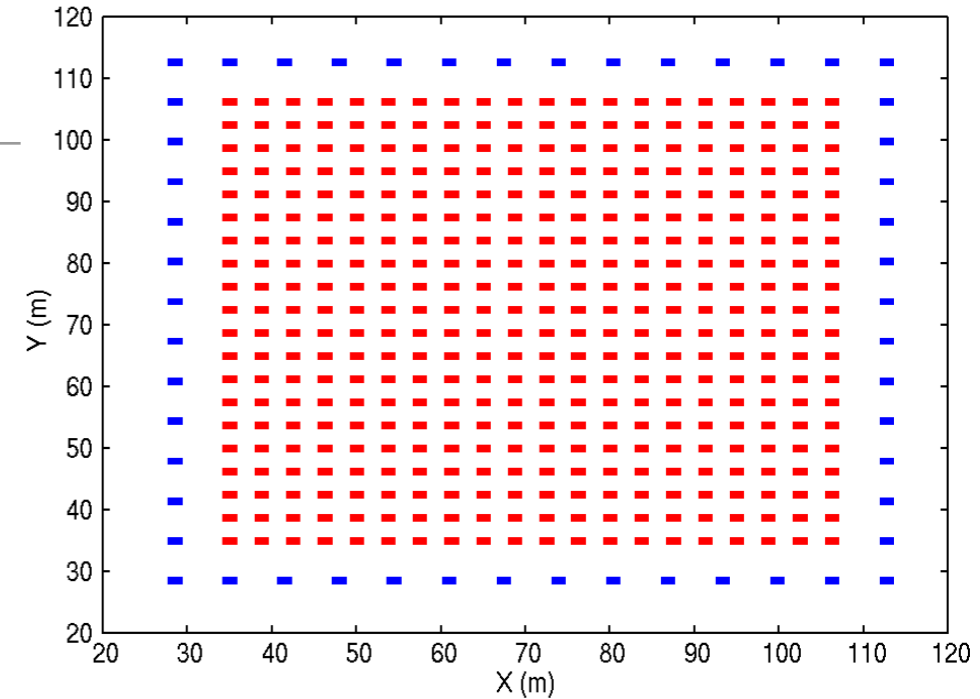
Tibet AS γ , 606 gm²

- 425 close-packed array of **burst detectors**, located near the centre of the array, for the detection of high energy secondary particles in the **shower core region**.

Burst Detector



The burst detectors observe the electron size (**burst size**) under the lead plate induced by high energy e.m. particle in the shower core region



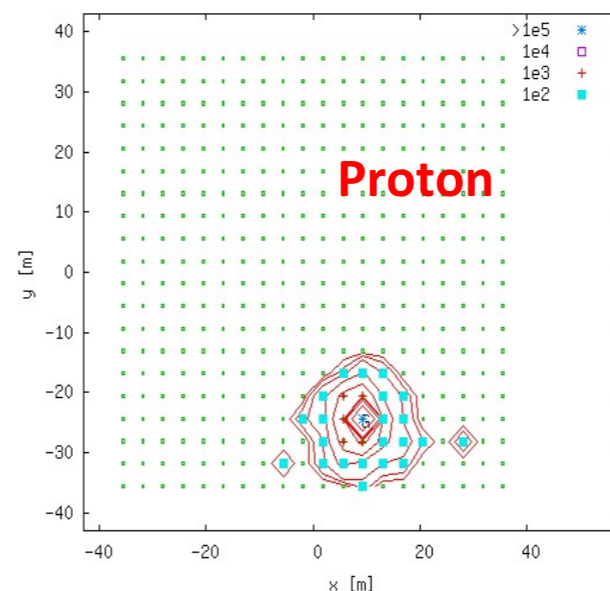
- Number of SCD: 0.5 m² x 452
- Cover Area: 5170 m²
- Energy region: 30 TeV - 10 PeV
- Core position resolution: 1.5 m @50 TeV

Each burst detector is constituted by 20 optically separated scintillator strips of 1.5 cm × 4 cm × 50 cm read out by two PMTs operated with different gains to achieve a wide dynamic range (1- 10⁶ MIPs).

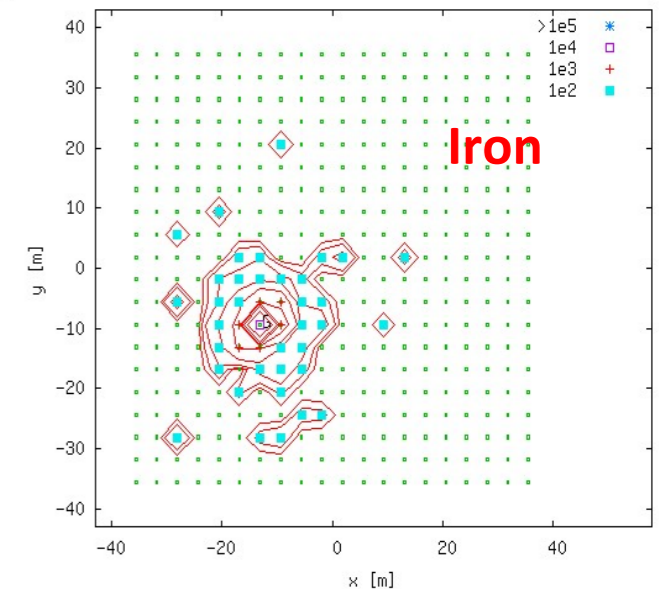


- Lead plate (80 cm X 50 cm X 7 rl)
- Iron plate (1 m X 1 m X 1 rl)

Q= 1 E0=4.4E+06 Ne=2.8E+06 s= 1.13 Z= 0.86 Nb=1.3E+05 Top=1.1E+07

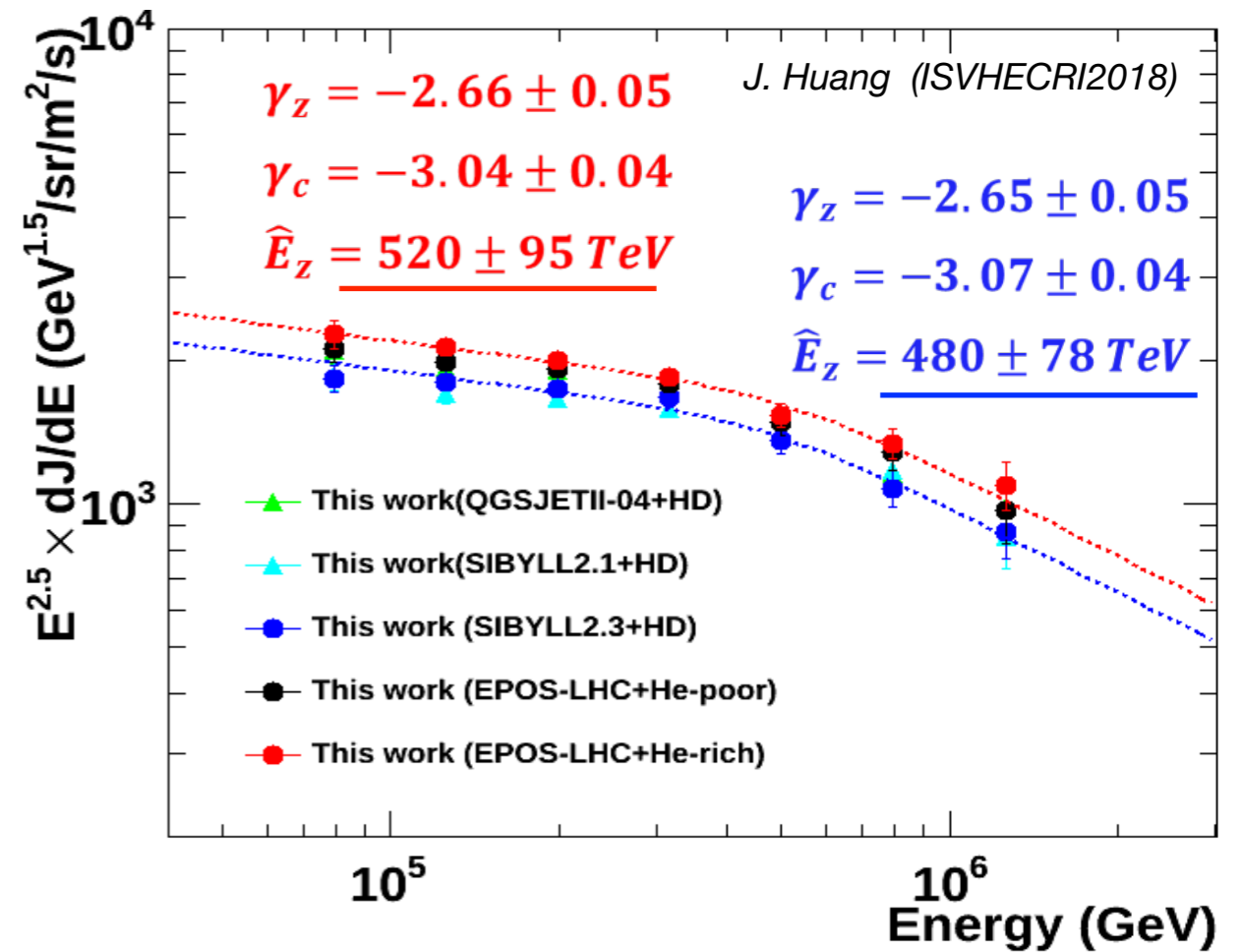
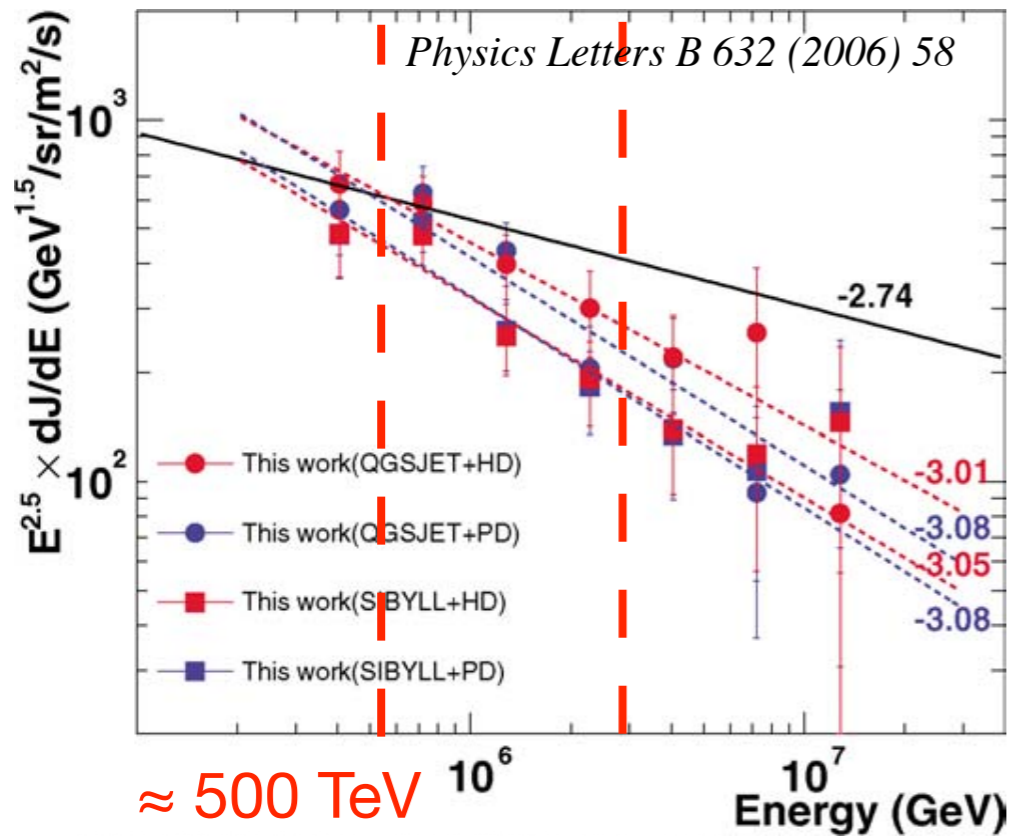


Q=26 E0=6.4E+06 Ne=2.8E+06 s= 1.19 Z= 0.95 Nb=6.4E+04 Top=4.5E+04

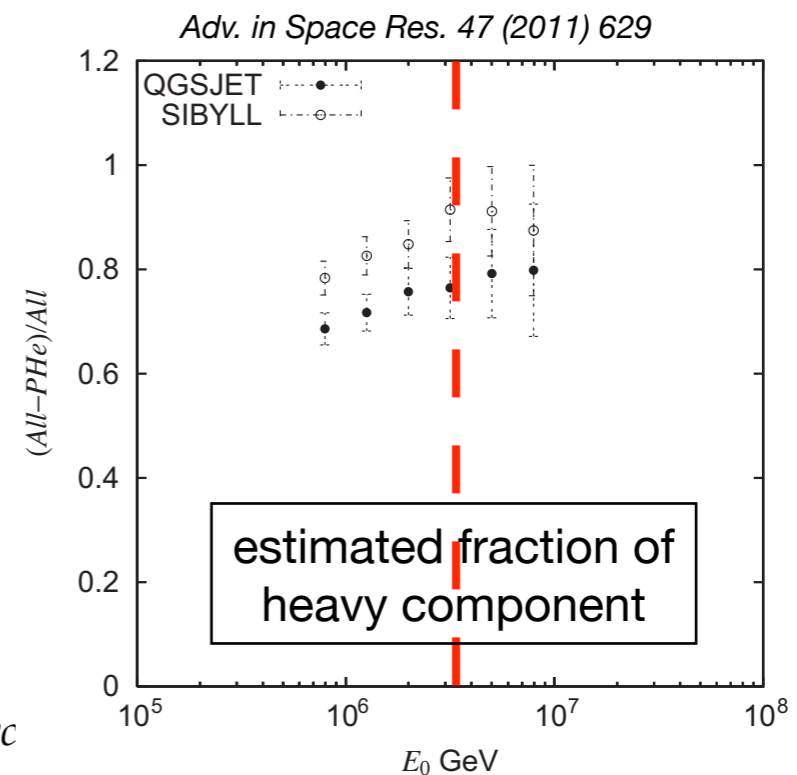


Composition at the knee: Tibet AS γ

Separation based on shower core study
(burst detectors)



- (1) The power index is steeper than that of all-particle spectrum before the knee, suggesting that the light component has the break point at lower energy than the knee.
- (2) The fraction of the light component to the all-particles is less than 30% which tells that the main component responsible for the knee structure is heavier than helium.



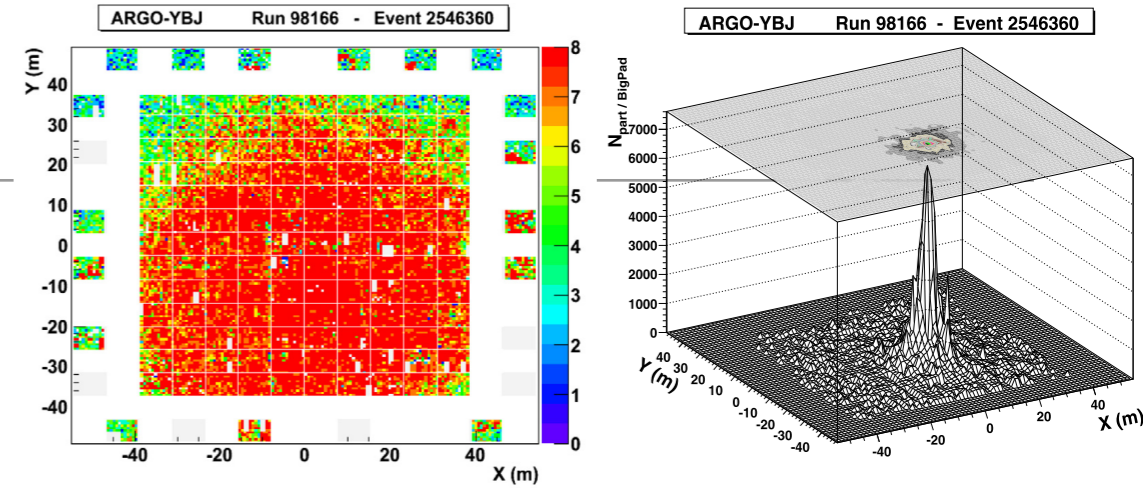
Astrophys. Space Sci. Trans., 7 (2011) 15

ARGO-YBJ, 606 g/cm²

Linearity up to several 10⁴/m² (→ ≈ 10 PeV)

Core resolution ≈ 1 m

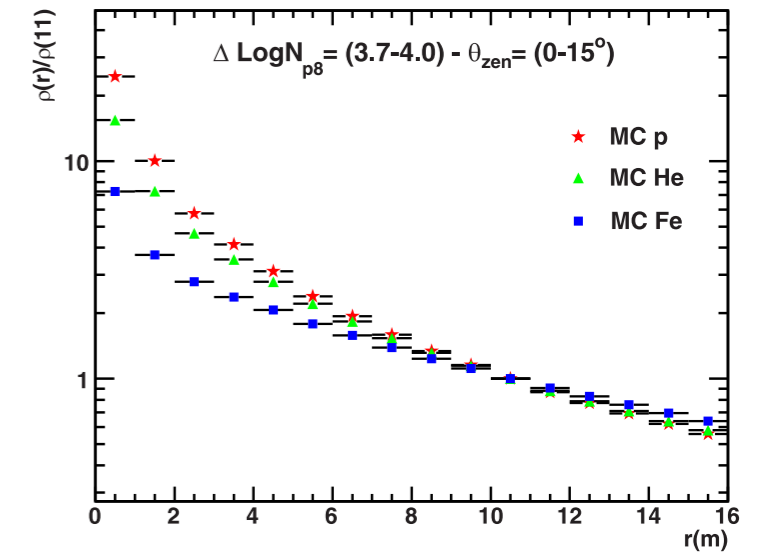
Estimator of the primary CR energy: N_{p8} , *the number of particles detected within a distance of 8 m from the shower axis*



→ *very forward region!*

Lateral distribution up to 10 m from the core described with a NKG-like function

$$\rho(r) = A \cdot \left(\frac{r}{r_0}\right)^{s'-2} \cdot \left(1 + \frac{r}{r_0}\right)^{s'-4.5} \quad s' = \text{lateral age}$$



Astrop. Physics. 93 (2017) 46

s' reflects the developing stage of the shower, being a detected p-induced shower on average younger (which implies a smaller s' value) than a shower induced by an iron nucleus

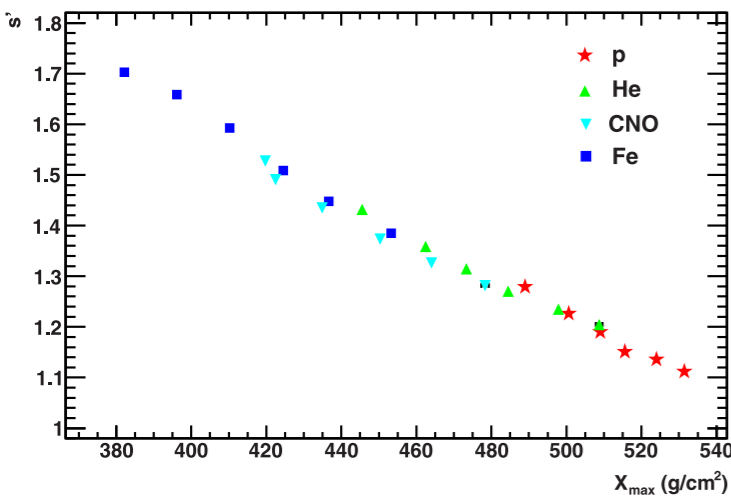
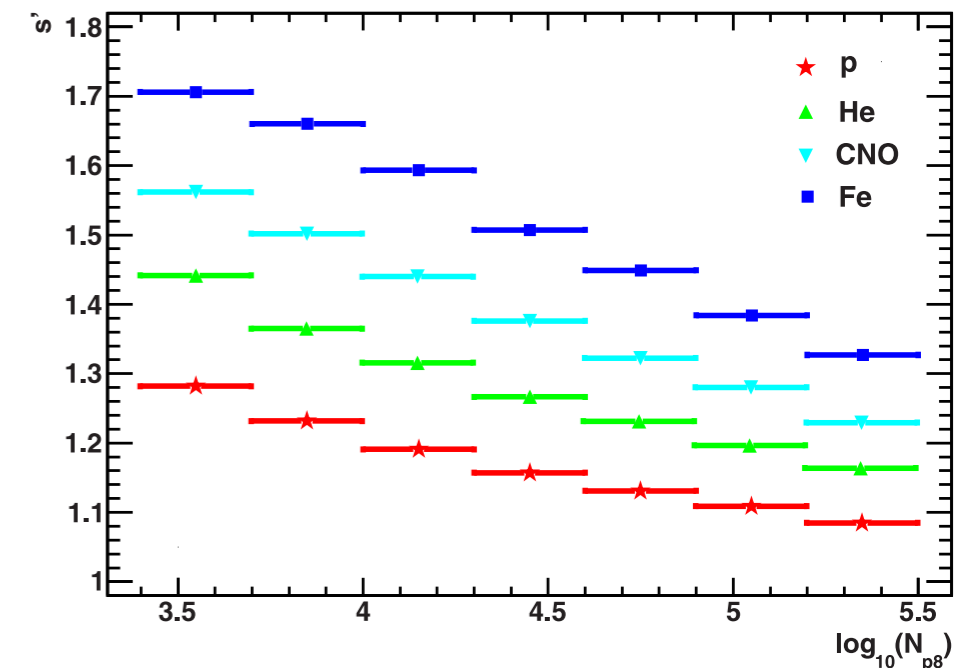


Fig. 11. The average lateral age parameter s' resulting from the fits of the lateral particle distributions in single events of simulated p, He, CNO group and Fe samples (in each N_{p8} bin, see text) vs the corresponding X_{\max} average values. Only near-vertical showers ($\theta < 15^\circ$) are considered.

'universality property' of the detected shower development in the atmosphere: the shape parameter s' depends only on the development stage of the shower, independently from the nature of the primary particle and energy



ARGO-YBJ, 606 g/cm²

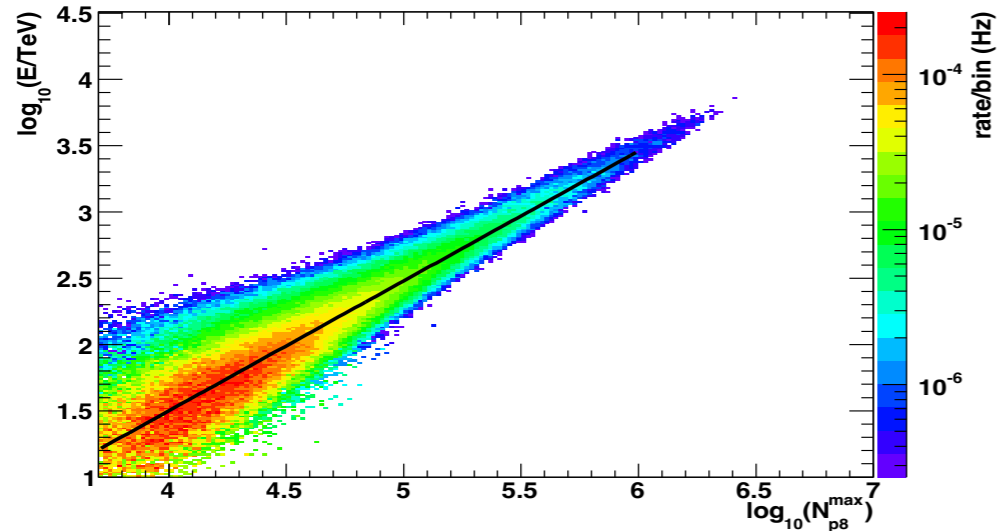


FIG. 5: Two-dimensional histogram of $\log_{10}(E/\text{TeV})$ vs $\log_{10}(N_{p8}^{\text{max}})$ for a simulated mixture of quasi-vertical ($\theta < 15^\circ$) H, He, CNO group and Fe nuclei, in the assumption of Hörandel composition model. A linear fit is superimposed.

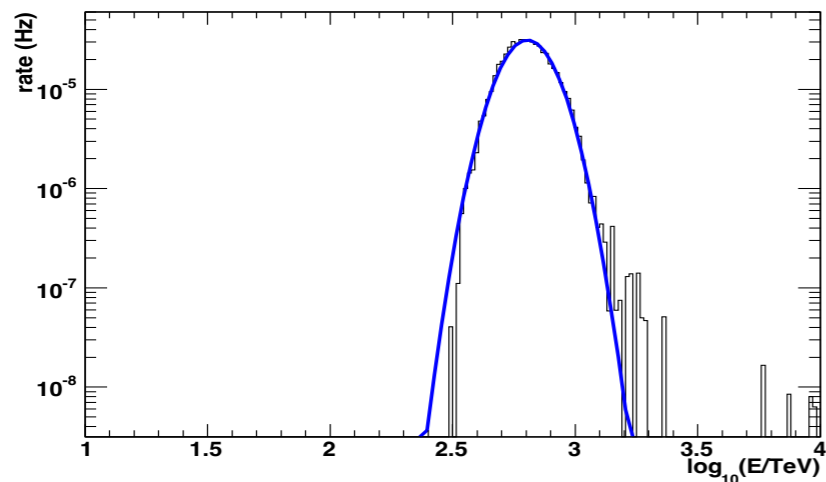


FIG. 6: The \log_{10} of energy distribution corresponding to the interval of the truncated size at maximum $\log_{10}(N_{p8}^{\text{max}}) = [5.30, 5.38]$, just as an example. As shown, the distribution is properly fitted by a Gaussian function.

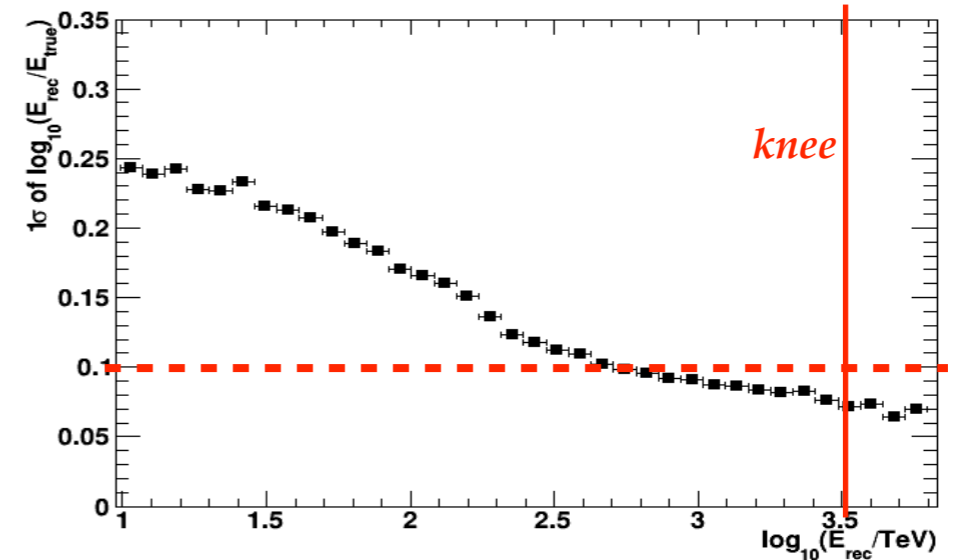


FIG. 7: Energy resolution as a function of the reconstructed energy E_{rec} for quasi-vertical events ($\theta < 15^\circ$), $\lambda_{\text{abs}} = 100 \text{ g/cm}^2$ and Hörandel model [13]. The method was applied for $E \geq 100 \text{ TeV}$.

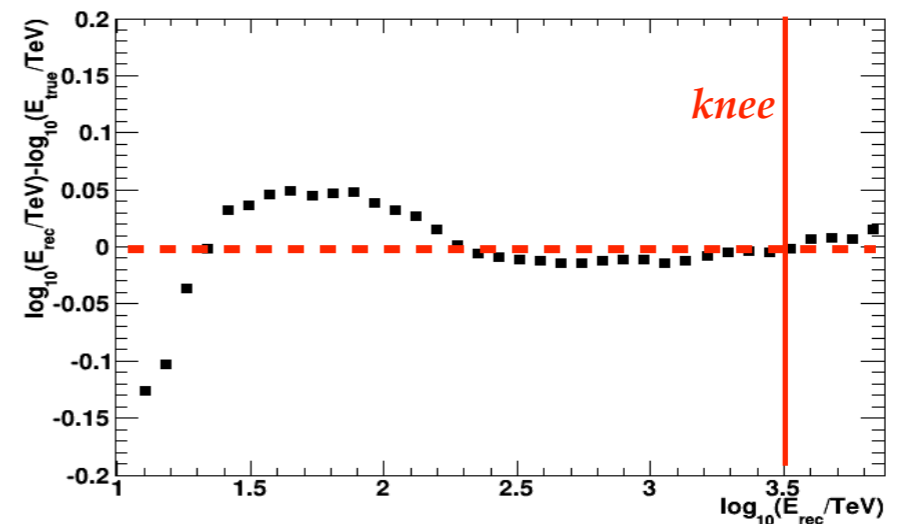
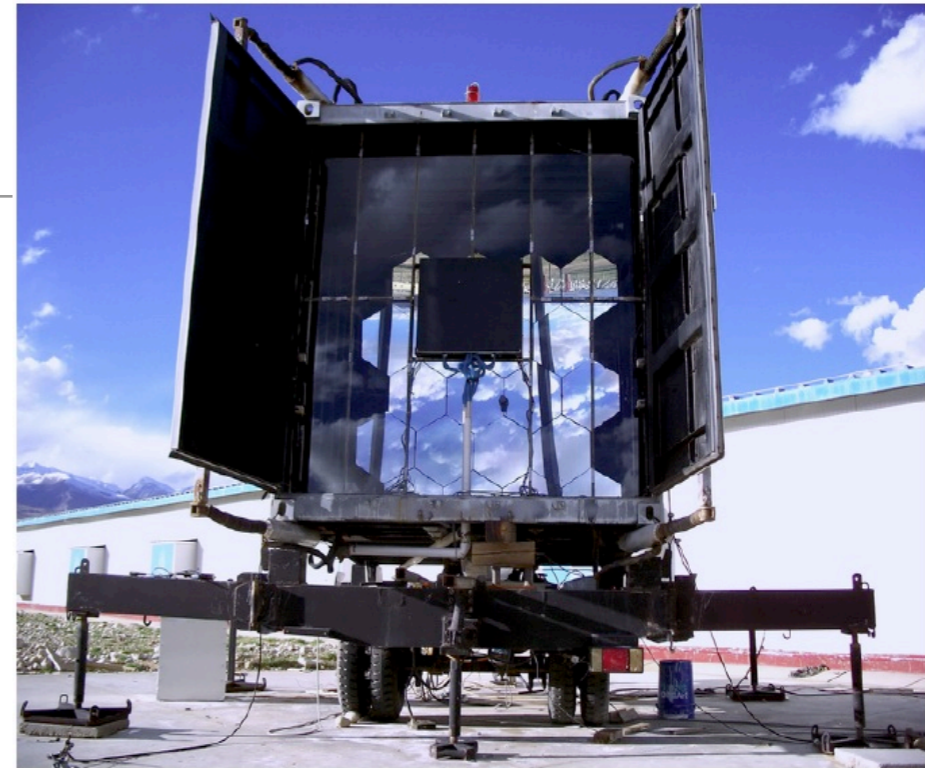


FIG. 8: Energy calibration bias as a function of the reconstructed energy E_{rec} for quasi-vertical events ($\theta < 15^\circ$), $\lambda_{\text{abs}} = 100 \text{ g/cm}^2$ and Hörandel model [13]. The method was applied for $E \geq 100 \text{ TeV}$.

ARGO-YBJ + WFCTA

A prototype of the future LHAASO telescopes has been operated in combination with ARGO-YBJ

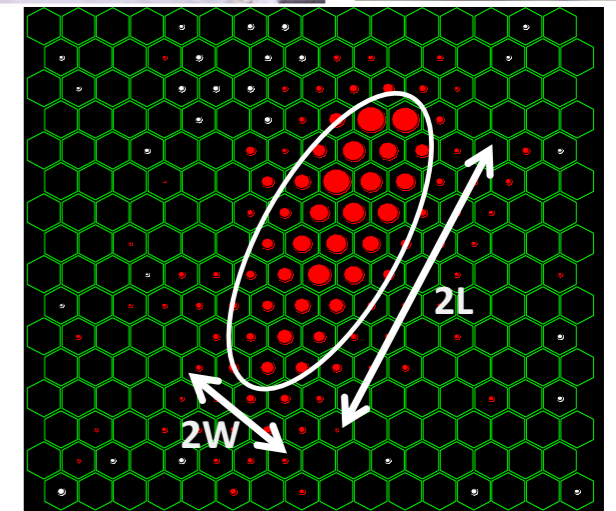
- 4.7 m² spherical mirror composed of 20 hexagon-shaped segments
- 256 PMTs (16 × 16 array)
- 40 mm Photonis hexagonal PMTs (XP3062/FL)
- pixel size 1°
- FOV: 14° × 14°
- Elevation angle: 60°



Phys. Rev. D 92, 092005 (2015)

❖ **ARGO-YBJ:** core reconstruction

the largest number of particles N_{max} recorded by a RPC in an given shower, i.e. the particle density within 3 m from the core position.

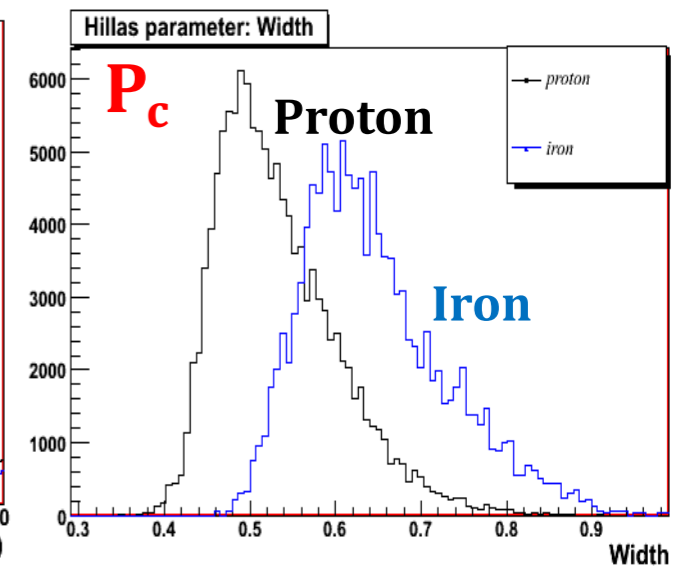
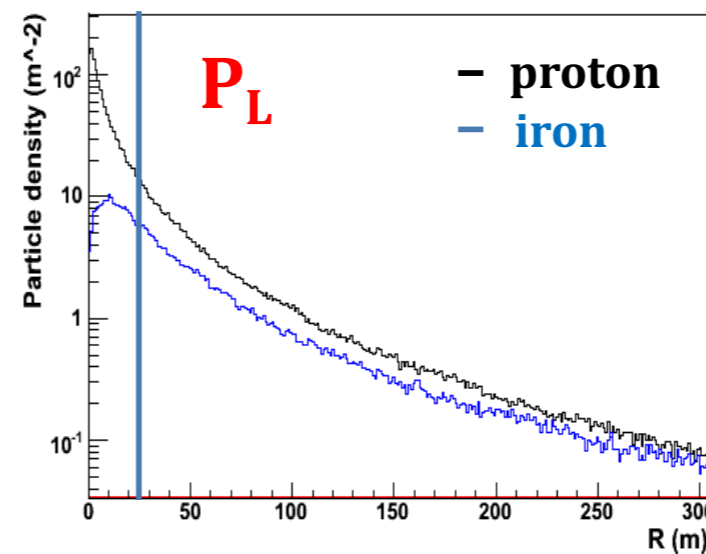


❖ **Cherenkov telescope:** longitudinal information

Hillas parameters → mass sensitive

Energy reconstruction

- angular resolution: 0.2°
- shower core position resolution: 2 m



Elemental composition and kinematic regions

All experiments observing a proton knee well below the PeV used observables exploring the **(very) forward region** of the hadronic interaction undergone by the primary cosmic ray.

All experiments observing a proton knee at a few PeV explored the **central region** (mainly with GeV muons).

EAS-TOP, 800 g/cm²

The cosmic ray primary composition in the “knee” region through the EAS electromagnetic and muon measurements at EAS-TOP

EAS-TOP Collaboration

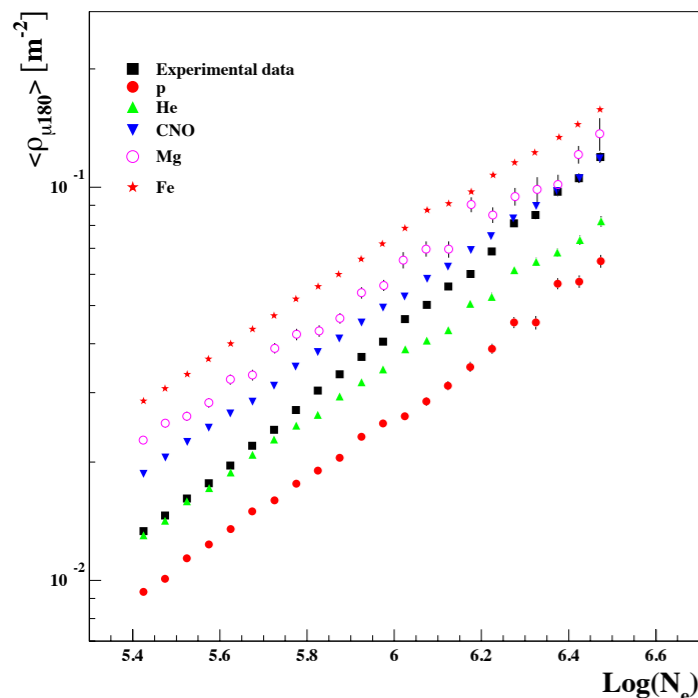
M. Aglietta ^{a,b}, B. Alessandro ^{b,*}, P. Antonioli ^c, F. Arneodo ^d, L. Bergamasco ^{b,e}, M. Bertaina ^{b,e}, C. Castagnoli ^e, A. Castellina ^{a,b}, A. Chiavassa ^{b,e}, G. Cini Castagnoli ^{b,e}, B. D’Ettorre Piazzoli ^f, G. Di Sciascio ^f, W. Fulgione ^{a,b}, P. Galeotti ^{b,e}, P.L. Ghia ^{a,d}, M. Iacovacci ^f, G. Mannocchi ^{a,b}, C. Morello ^{a,b}, G. Navarra ^{b,e}, O. Saavedra ^{b,e}, G.C. Trincherò ^{a,b}, S. Valchierotti ^{b,e}, P. Vallania ^{a,b}, S. Vernetto ^{a,b}, C. Vigorito ^{b,e}

Shower array

- 35 modules, 10 m² each, of plastic scintillators distributed over an area of 10⁵ m²
- 140 m² hadronic calorimeter (had >30 GeV, muons >1 GeV)
- 8 Cherenkov telescopes wide fov

Observables (central region):

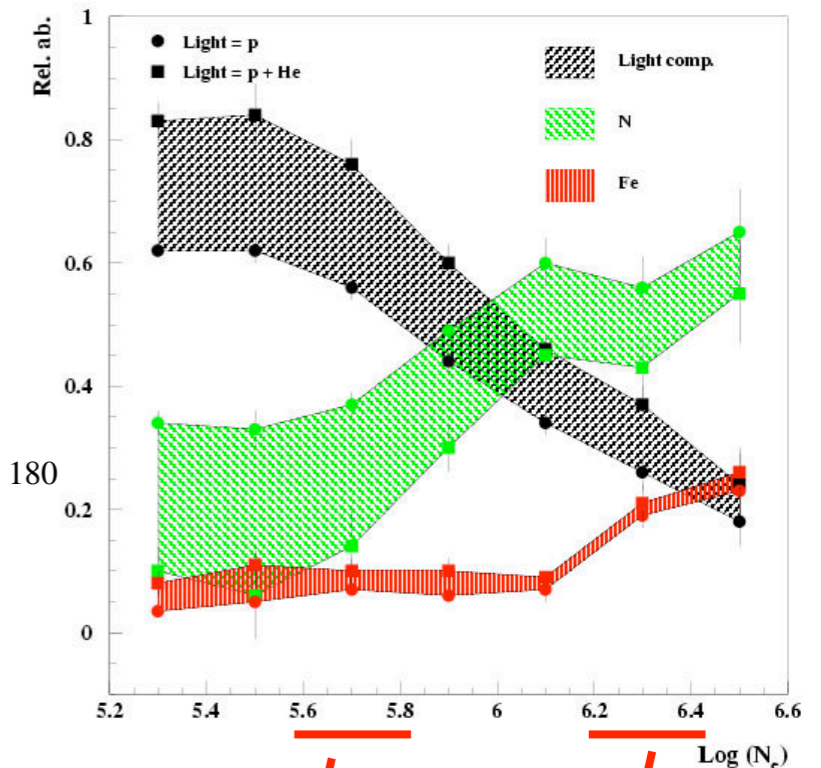
- the correlated muon size (N_{μ}) and shower size (N_e) spectra
- the evolution of the average $N_{\mu 180}$ and their distributions vs N_e
- the evolution of $\rho_{\mu 180}$ vs N_e



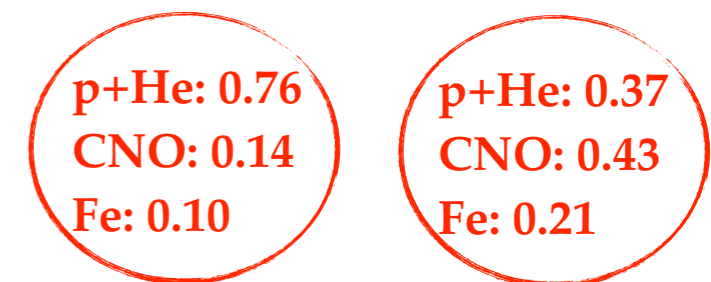
the number of muons $N_{\mu 180}$ and the muon density $\rho_{\mu 180}$ are measured between 180 and 210 m from the core

Conclusions.

- Steep spectrum of the light mass group $\gamma_{p+He} > 3.1$
- Helium primaries dominates at the knee:
 $E_k^{He} \approx (3.5 \pm 0.3) \times 10^6 \text{ GeV}$
- Possible knee of CNO mass group:
 $E_k^{CNO} \approx (6 - 7) \times 10^6 \text{ GeV}$
- Constant slope of the heavy component



Relative abundances



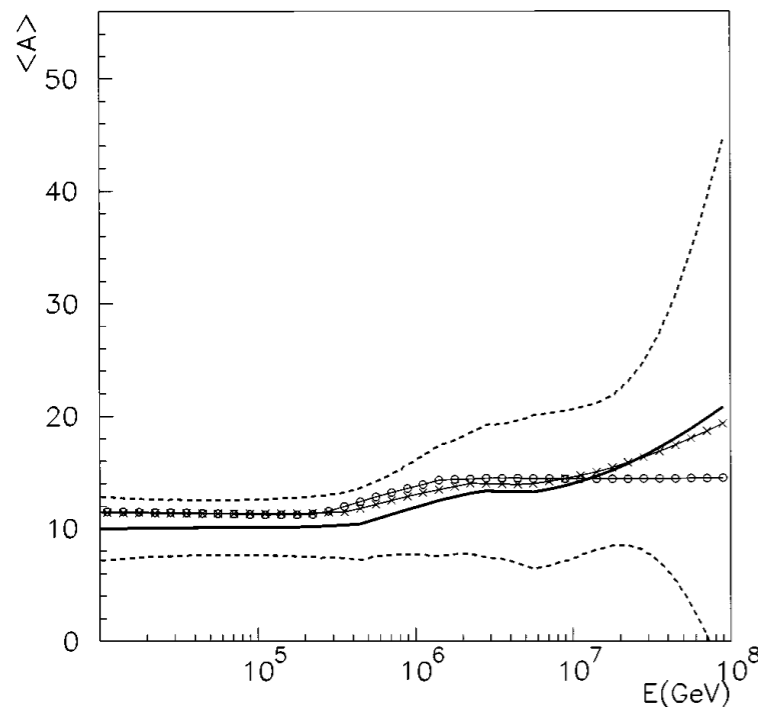
Astrop. Physics. 21 (2004) 583

MACRO, TeV muons

Muons underground $E_\mu \geq 1.3 - 1.8$ TeV

Such muons originate from the decays of mesons produced in the first interactions of the incident primary in the atmosphere, and thus are from a quite different rapidity region than the GeV muons usually used for such analyses ($x_F > 0.1, 0.2$ the rapidity region being $y - y_{beam} \approx - (4.5 - 5.0)$ at $\sqrt{s} \approx 10$ TeV)

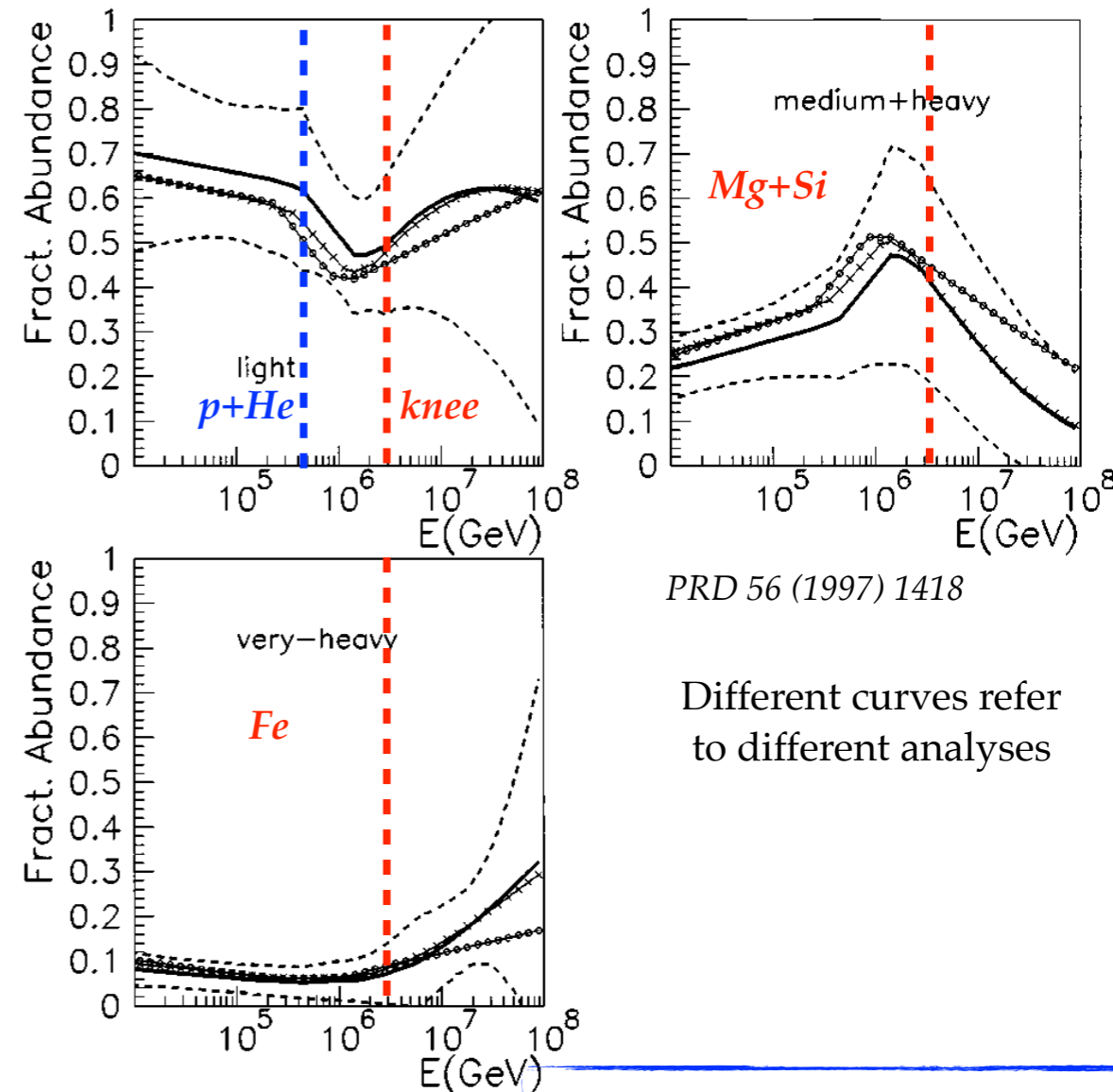
The experiment provides data related to the first stages of the shower development, from secondaries produced *beyond the central rapidity region*.



$\langle A \rangle$ shows little dependence on the primary energy below ~ 1000 TeV.

Fine structures are missing!

$\langle A \rangle$ is not sensitive to composition details



PRD 56 (1997) 1418

Different curves refer to different analyses

Possible knee of the light component at ≈ 500 TeV

MACRO, TeV muons

Underground multiple TeV muons come from different kinematical regions determined by the energy of their parents.

Multimuon events originating from *less energetic primaries* are preferentially produced from parents in the *very forward fragmentation region*, whereas at higher primary energies the corresponding production kinematical region is at lower x_F .

In particular it can be recognized that the *highest x_F parents* are the main contributors of the *low multiplicity muon events* and then largely determine the inclusive muon rates.

$$\langle x_{lab} \rangle \text{ is the laboratory energy fraction in the forward direction } \sim x_F \sim \frac{E_\pi}{E_0}$$

$$\langle E_\pi \rangle = \frac{\gamma + 2}{\gamma + 1} E_\mu^{thr} \frac{1 - r_\pi^{(\gamma+1)}}{1 - r_\pi^{(\gamma+2)}} \simeq 1.7 \text{ TeV} \quad \text{If } E_\mu^{thr} \simeq 1.3 \text{ TeV} \quad \text{where } r_\pi = \frac{m_\pi^2}{m_\mu^2}$$

For “low” E_0 values (a few TeV) $\langle x_{lab} \rangle \sim 1$, i.e. in the very forward region.

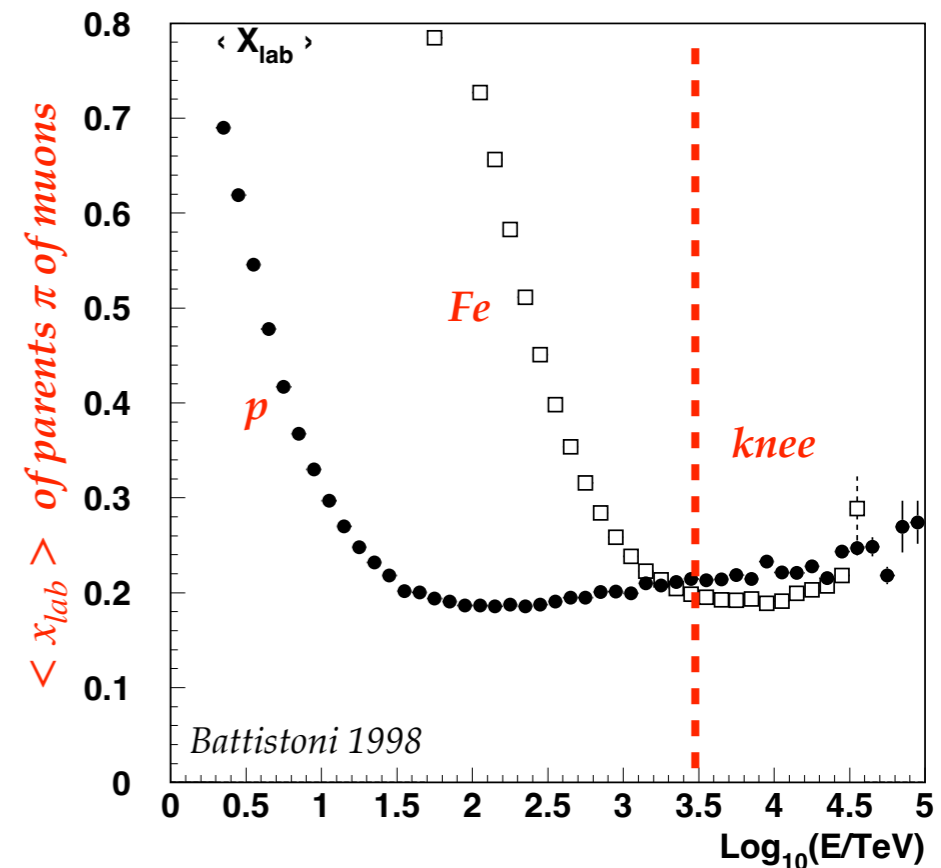
In that cases, only muons from the first generation in the cascade are detected, and the primary interaction is really investigated.

A low EAS-TOP trigger allowed to select (protons) events in the range 50-100 TeV. A coincidence with MACRO in principle allows to investigate *interaction models in the fragmentation region.*

PRD 56 (1997) 1418

E (TeV)	$N_\mu=1$	$N_\mu=2-4$	$N_\mu \geq 5$
< 10	0.41	0.34	
$10-10^2$	0.25	0.19	0.09
10^2-10^3	0.23	0.19	0.16
10^3-10^4	0.22	0.20	0.18
10^4-10^5	0.20	0.20	0.19

Average x_F of the parent of the muons at MACRO depth, in different ranges of primary energy forward region $x_F > 0.2$



EAS-TOP + MACRO

The observables are the air shower size (N_e) measured by EAS-TOP and the TeV muon number (N_μ) recorded by MACRO.

TeV muons are produced in the early stages of the shower development and in a kinematic region quite different from the one relevant for the usual $N_\mu - N_e$ studies with shower arrays.

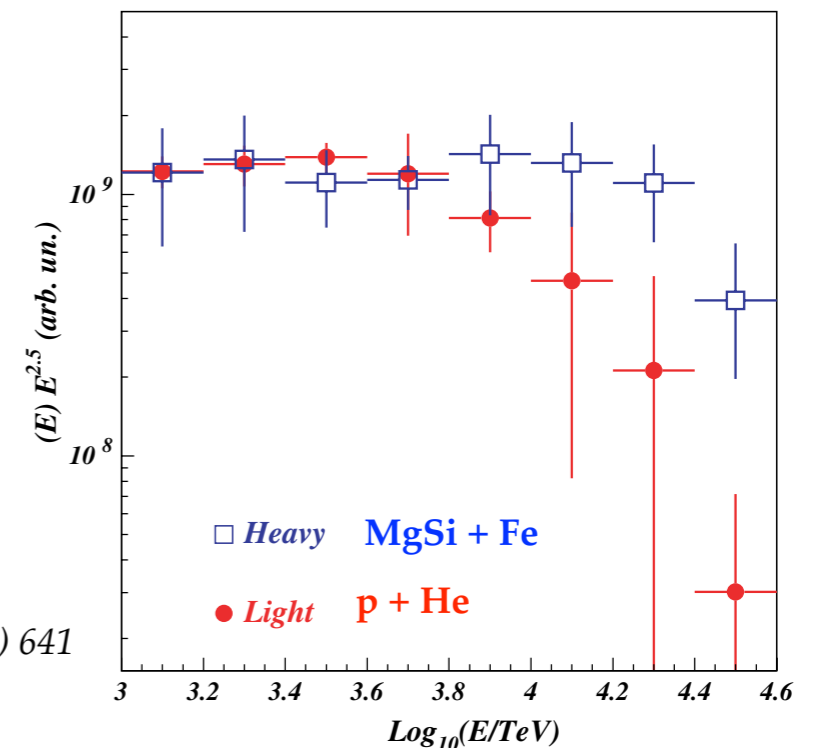
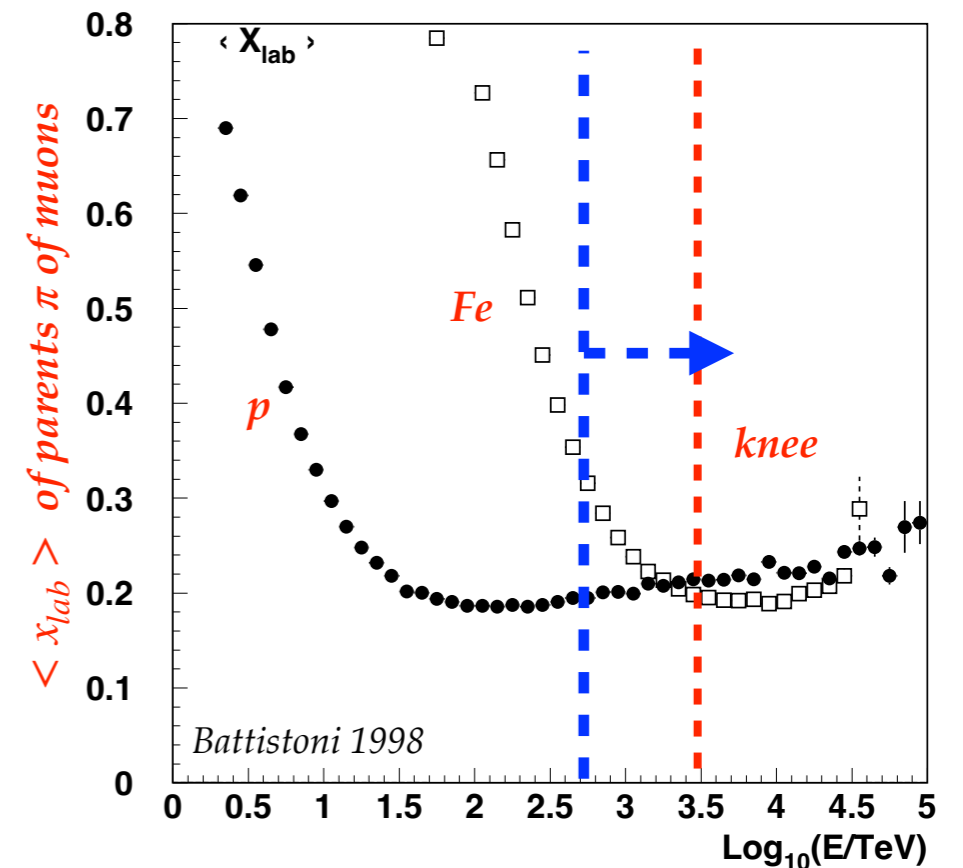
This analysis selected coincidence events coming from showers initiated by primaries having $E \geq 100$ TeV/nucleon where TeV muons mostly correspond to mesons produced between the central and fragmentation region (*at the edges of the fragmentation region, rather than in the central one*).

$\text{Log}_{10}(N_e)$ window	p_L	p_H
5.20–5.31	0.74 ± 0.07	0.26 ± 0.11
5.31–5.61	0.70 ± 0.05	0.30 ± 0.09
<i>knee</i> 5.61–5.92	0.66 ± 0.09	0.34 ± 0.14
→ 5.92–6.15	0.50 ± 0.17	0.50 ± 0.24
6.15–6.35	0.30 ± 0.20	0.70 ± 0.32
6.35–6.70	0.24 ± 0.32	0.76 ± 0.45

We concluded that the results do not depend on the production region kinematics

But (very) forward region not investigated yet

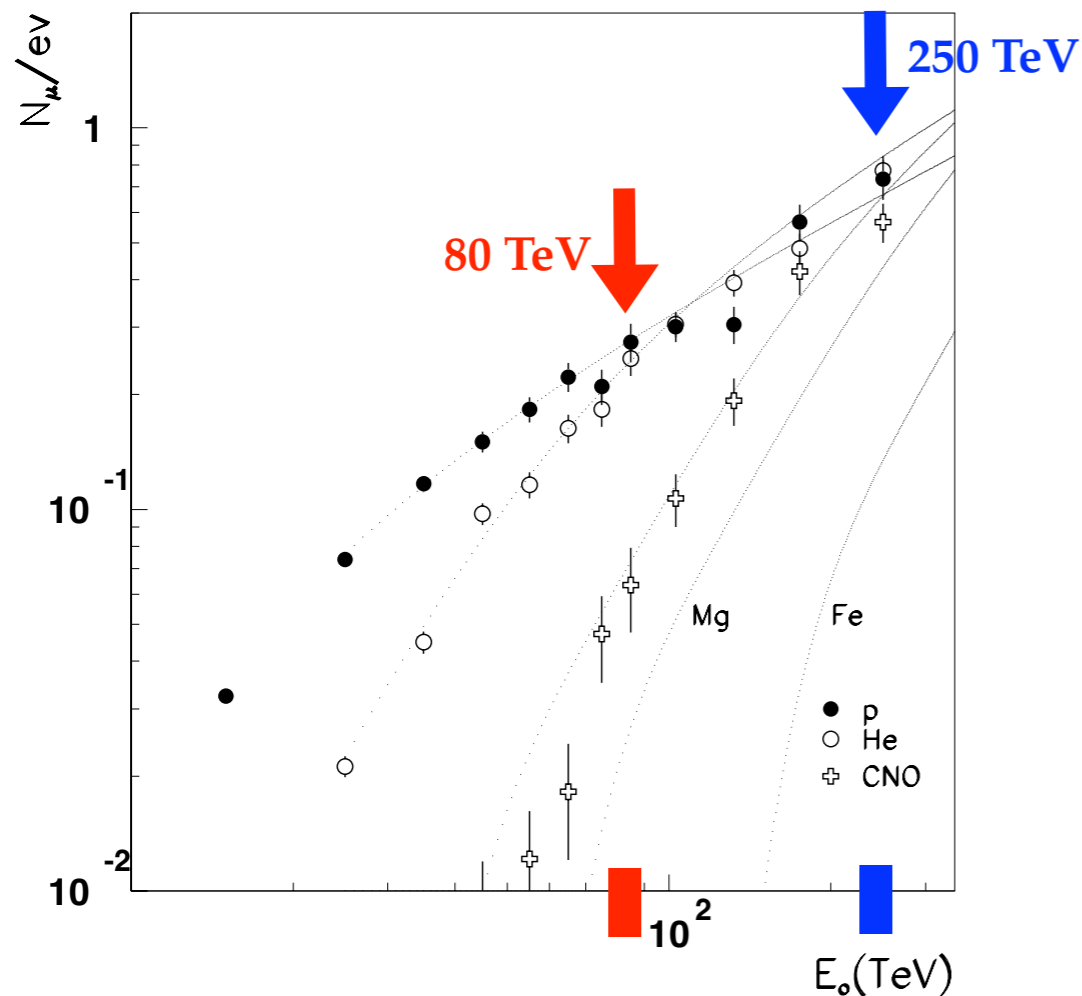
Astrop. Physics. 20 (2004) 641



EAS-TOP Cherenkov + MACRO TeV muons

- The primary proton spectrum in the energy range 0.5–50 TeV has been deduced from the hadron spectrum measured in the EAS-TOP calorimeter.
- The fraction of He and CNO primaries is obtained from the atmospheric Cherenkov light density measurements at different distances at ground (proportional to the total energy of the primary) combined with the TeV muons recorded by MACRO

Astrop. Physics. 21 (2004) 223



Beams are well defined:

- **p** at $E_0 < 50$ TeV
- **p+He** at $50 < E_0 < 100$ TeV
- **p+He+CNO** at $E_0 > 100$ TeV

- **At $E \approx 80$ TeV** $N_{\mu}^p \approx N_{\mu}^{He}$
- **At $E \approx 250$ TeV** $N_{\mu}^p \approx N_{\mu}^{He} \approx N_{\mu}^{CNO}$

Same efficiency (inside 15%) in TeV muon production
Relative abundances are not distorted

Number of muons per event reaching the MACRO depth, protons, He and CNO vs primary energy

EAS-TOP Cherenkov + MACRO TeV muons

Astrop. Physics. 21 (2004) 223

The shower and its geometry are selected through the muons detected deep underground by MACRO ($E_\mu > 1.3$ TeV).

The lateral distribution of Cherenkov light is measured to select proton and helium primary beam at 2 core distances $r < 50$ and $125 < r < 185$ m

The shape of the lateral distribution reflects the rate of energy release in the atmosphere (i.e., *the properties of the interaction*, the primaries being *dominated by the lightest components due to the TeV muon trigger requirement*).

Observables investigate *the region beyond the fragmentation region*

The obtained ratio $\frac{J_p}{J_p + J_{He}}$ (80 TeV) = 0.29 ± 0.09 implies that *around 100 TeV the helium flux dominates over the proton one.*

From the ratio $\frac{J_{p+He}}{J_p + J_{He} + J_{CNO}}$ (250 TeV) = 0.78 ± 0.17 it results that *CNO could provide a significant contribution to the flux in the 100–1000 TeV energy region*

The ratio of the 3 components at 250 TeV:

$$J_p : J_{He} : J_{CNO} = (0.20 \pm 0.08) : (0.58 \pm 0.19) : (0.22 \pm 0.17)$$

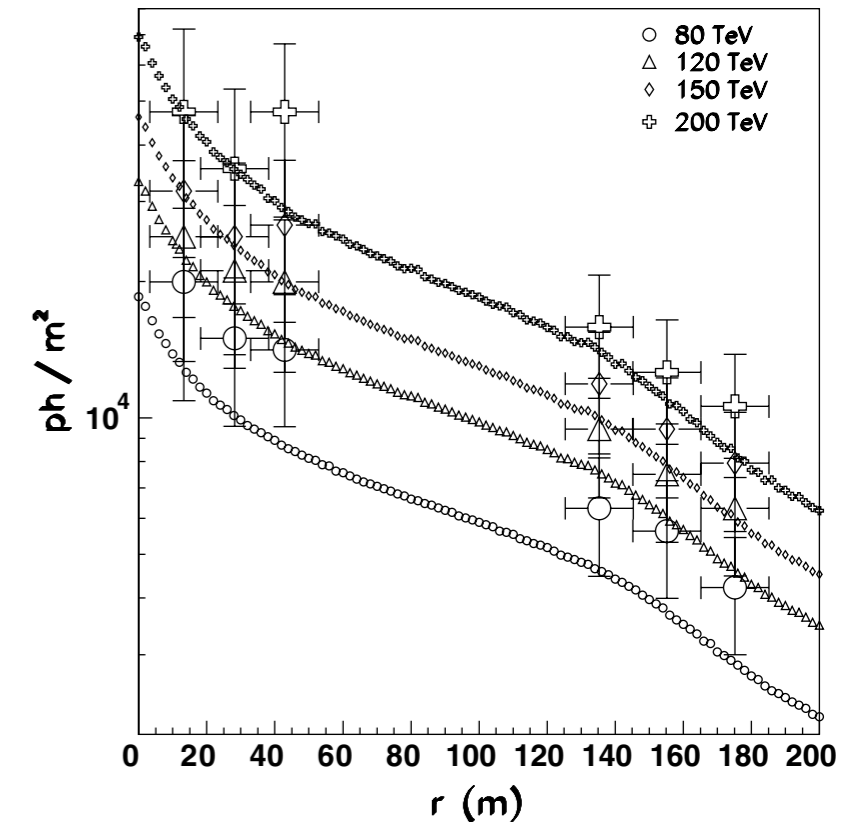


Fig. 13. Measured C.I. lateral distributions for 4 different shower energies, compared with the simulated ones using the JACEE spectra (i.e., energy–intensity relation).

“The data imply a decreasing proton contribution to the primary flux well below the observed knee in the primary spectrum.”

Shower Core and Very Forward region

h first interaction $\approx 15 - 20$ km a.s.l.

if $1 \leq r \leq 10$ m $\rightarrow \eta \approx 8 - 10$ at 5000 m asl

Very close to the leading, the most suitable way to investigate the atomic mass number of the primary CR.

The central region is dominated by contribution of younger sub-cascades started by pions produced at the late stage of EAS development and also their finite transverse momenta.

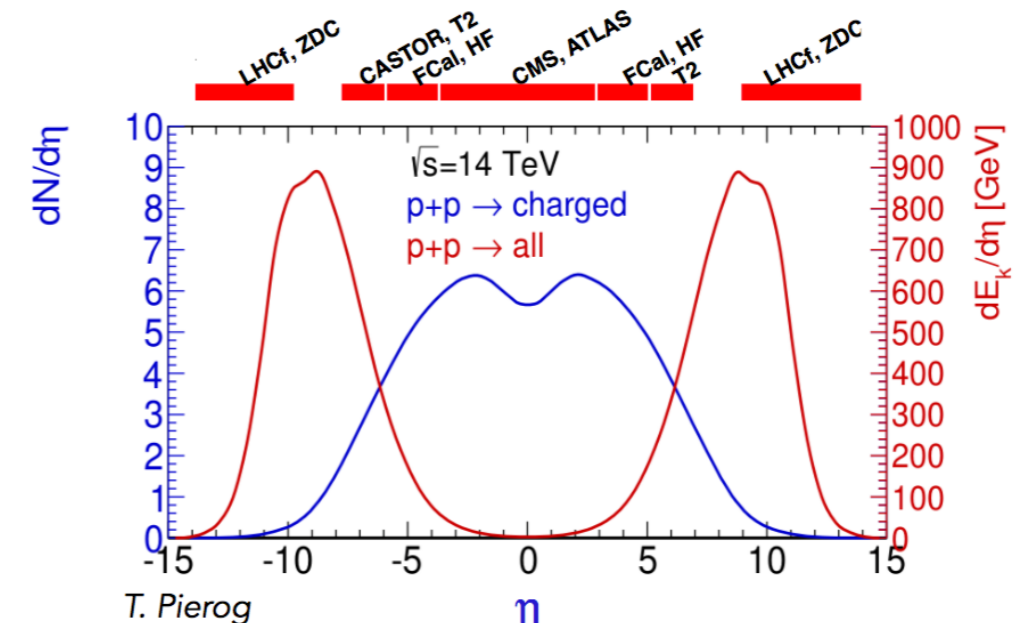
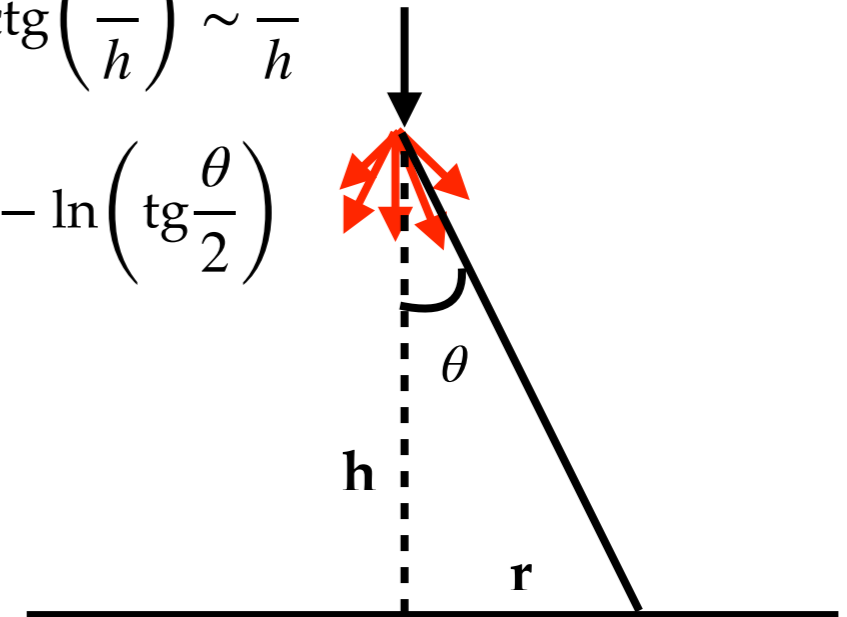
With increasing lateral distances the mean energy of pion interactions decreases

In the central region any distinctive features of fragmentation are smeared out by fluctuations in the large number of interactions, during development and propagation of EAS.

*Young showers \rightarrow p-like showers
High energy \rightarrow Young showers \rightarrow p-like showers*

$$\theta = \text{arctg}\left(\frac{r}{h}\right) \sim \frac{r}{h}$$

$$y \sim \eta = -\ln\left(\text{tg}\frac{\theta}{2}\right)$$

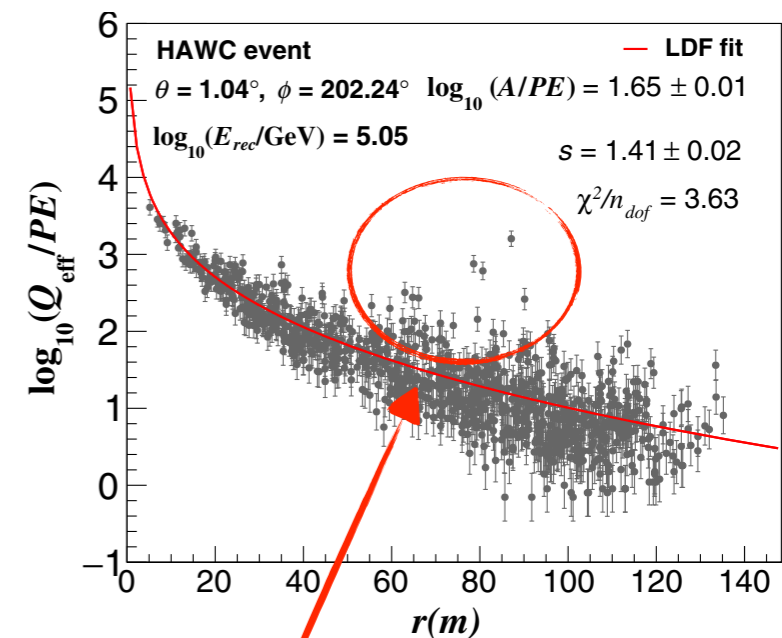
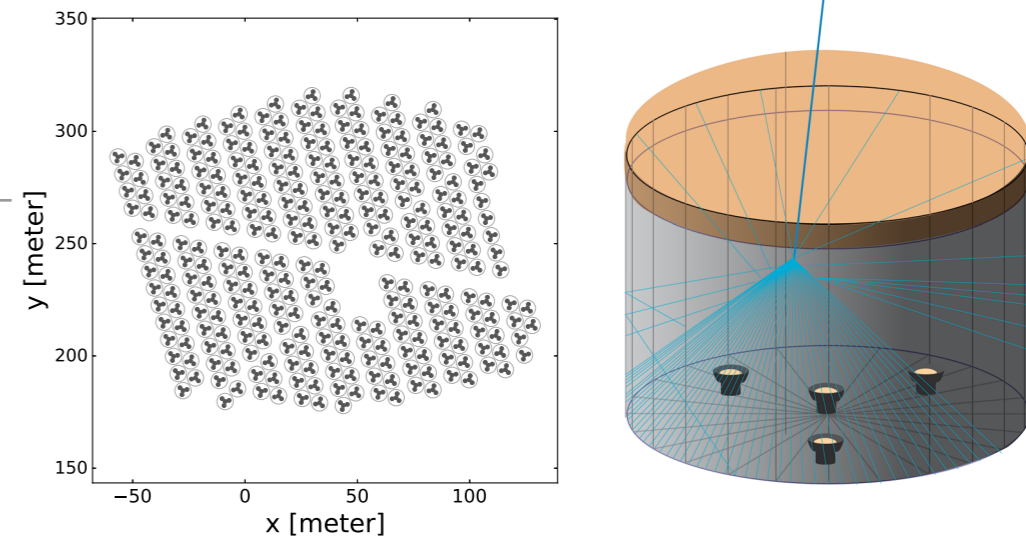


HAWC, 640 g/cm²

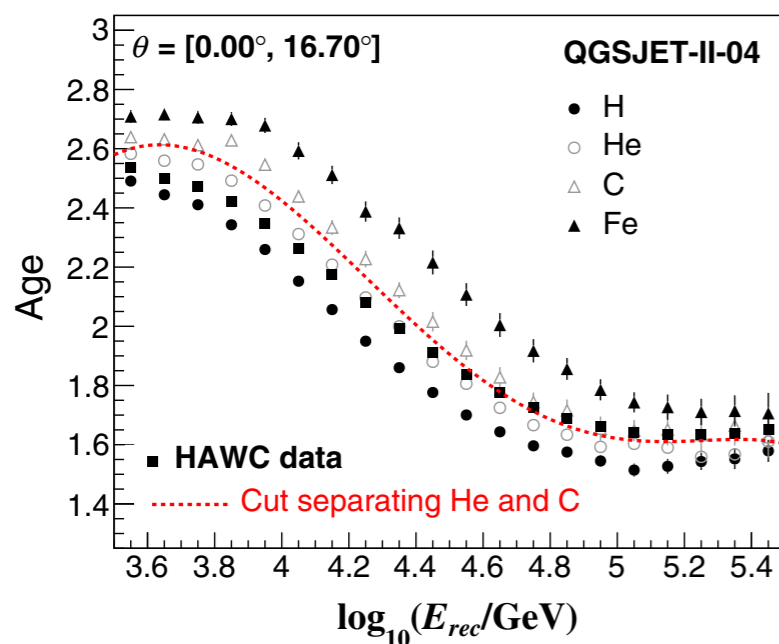
Mass separation is done *event-by-event* using an *energy dependent cut on the lateral shower age* parameter, derived from predictions of the QGSJET-II-04 model for different primary nuclei

On average, *heavy primaries tend to produce older showers* (large age values and flatter lateral distributions) *than light nuclei*, while high energy primaries create younger EAS (small values of age and steeper lateral distributions) than low energy ones.

*A cut on the effective charge at the PMT is applied ($Q_{eff} \leq 10^4$), not on the radial distance. Larger values of Q_{eff} are found close to the EAS core, hence, those points are removed. The region around the shower core that is excluded will depend on the shower size. Therefore, *the distance to the core increases with increasing energy.**



Outliers due to large and localised charge depositions from *muons*



From the fragmentation region to the central one approaching the PeV energy region

Conclusions

According to the measurements carried out by the experiments there is a (strong...?) evidence of a *possible role of the kinematic region* explored by the different observables.

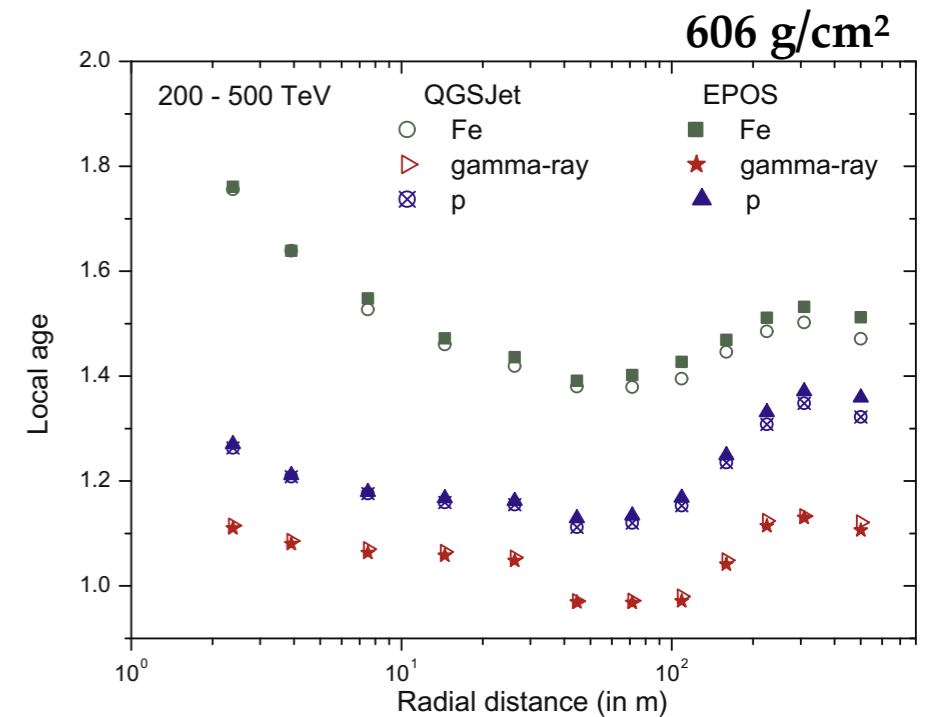
Is it possible that, in the central region, a combined effect between young showers from pions sub-showers and earlier showers produced by higher energy secondaries may mimic a light composition extending up to a few PeV?

As an example, the radial dependency of *the 'age' has little in common with the cascade theory depending on the superposition of younger sub-cascades*. We cannot predict this behavior with shower toy models.

Could LHAASO explore the (very) forward region where the bulk of primary energy is transferred deep in the atmosphere and investigate *possible effects of the kinematic regions on a measurement of the elemental composition?*

Probably this is the most interesting study that can be done in the PeV range

Unfortunately, it was never constituted a *working group* to investigate the reasons for these discrepancies unlike what was done between AUGER and TA.



R.K. Dey, *Astrop. Phys.* 44 (2013) 68



BASJE - MAS, 550 g/cm²

Since 1995 at **Chacaltaya, 5200 m asl**

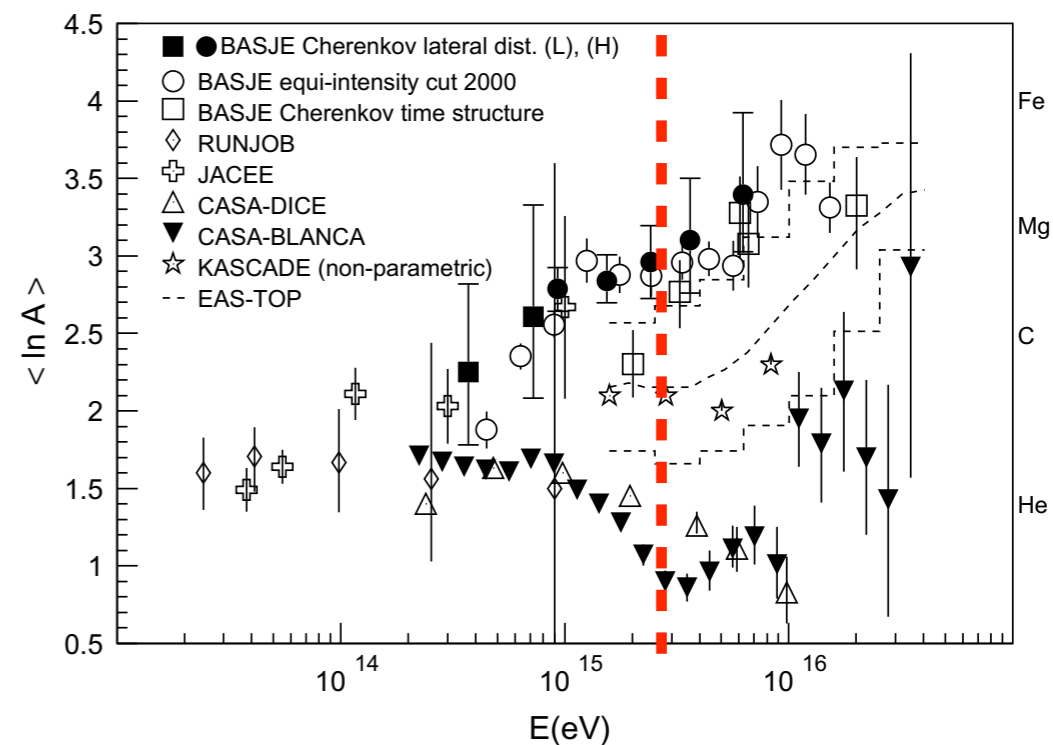
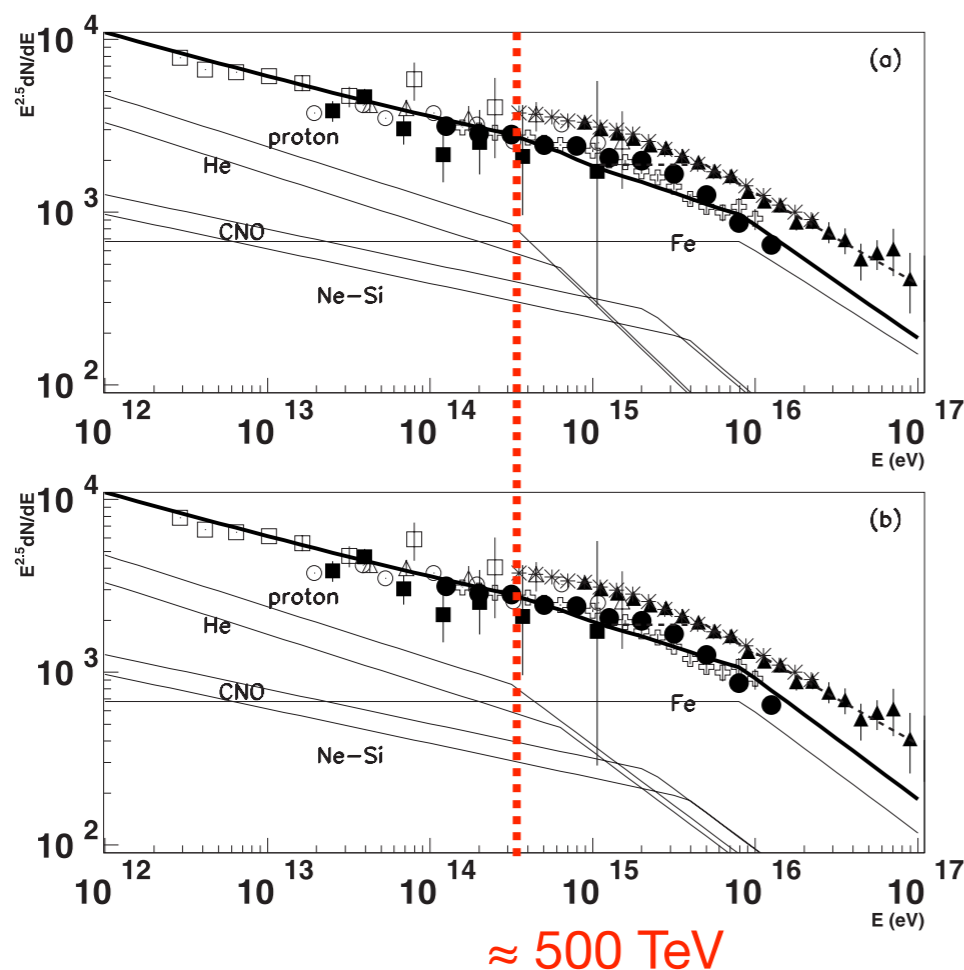
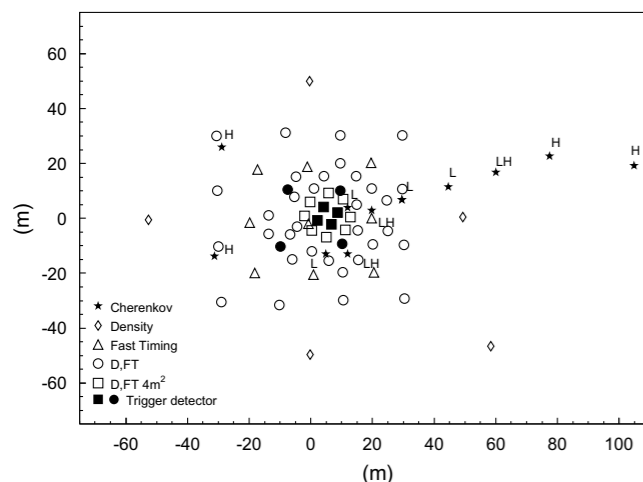
Astrop. Phys. 15 (2001) 357

ApJ 612 (2004) 268

Astrop. Phys. 29 (2006) 453

Different observables:

- *time structures of air Cerenkov light* to measure the EAS longitudinal developments at their early stages
- *EAS longitudinal developments* around their maxima and at later stages with an equi-intensity method analysis
- *lateral distributions of atmospheric Cerenkov photons*



higher than Carbon ($\ln A = 2.49$) at the knee

Different measurements are in agreement showing that *the dominant component around the knee is not protons.*

BASJE - MAS, 550 g/cm²

Time structures of air Cerenkov light associated with air showers to measure the EAS longitudinal developments at their early stages

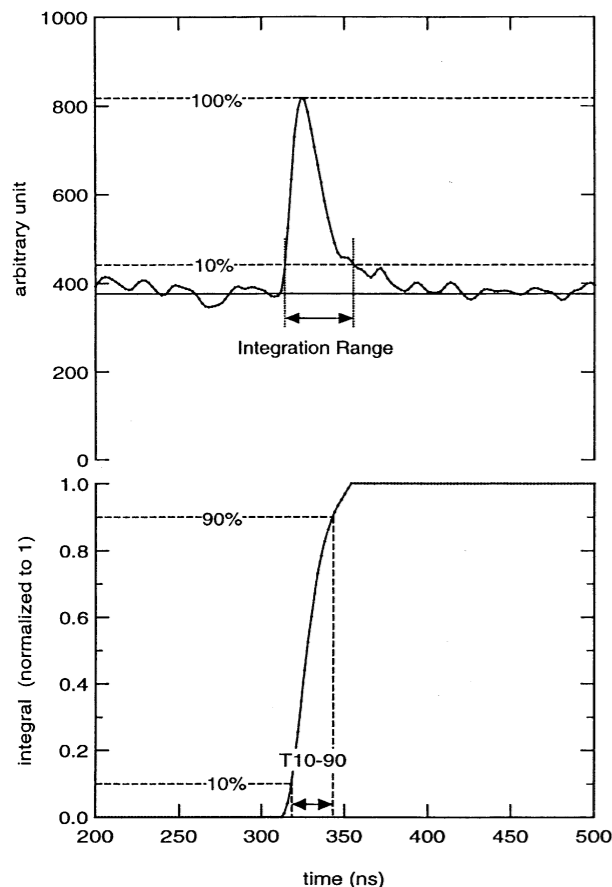


Fig. 8. Definition of the T_{10-90} .

The composition estimator T_{10-90} is defined as rise time of a time integrated pulse, and measured as a time interval between 10% and 90% of the full pulse height at large core distance.

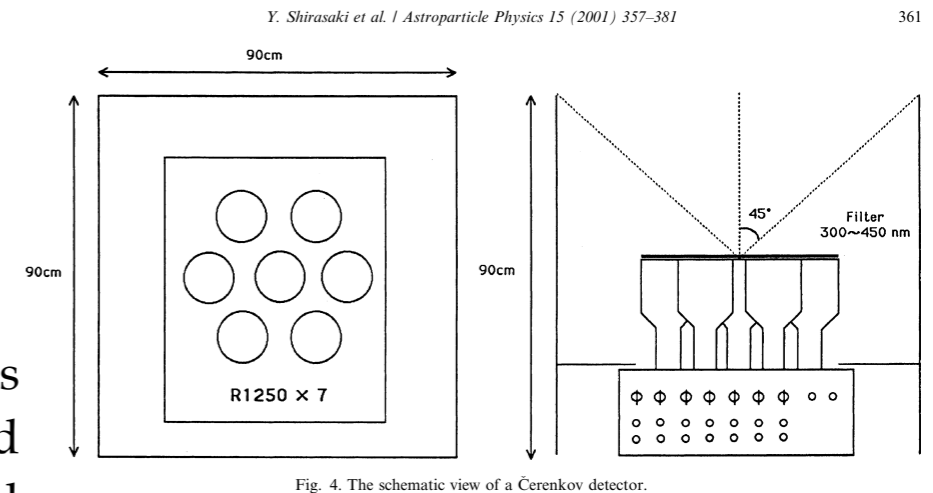
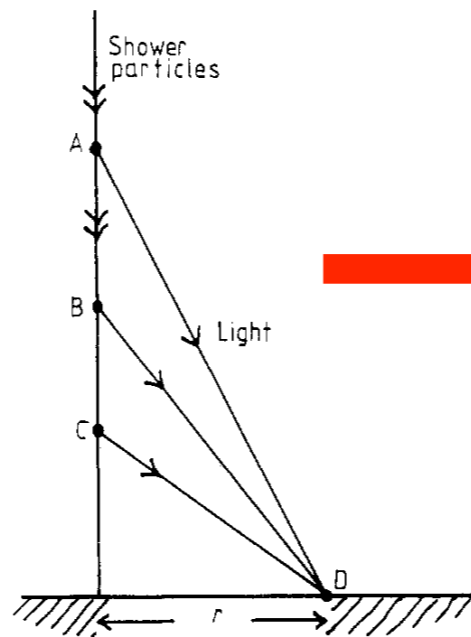
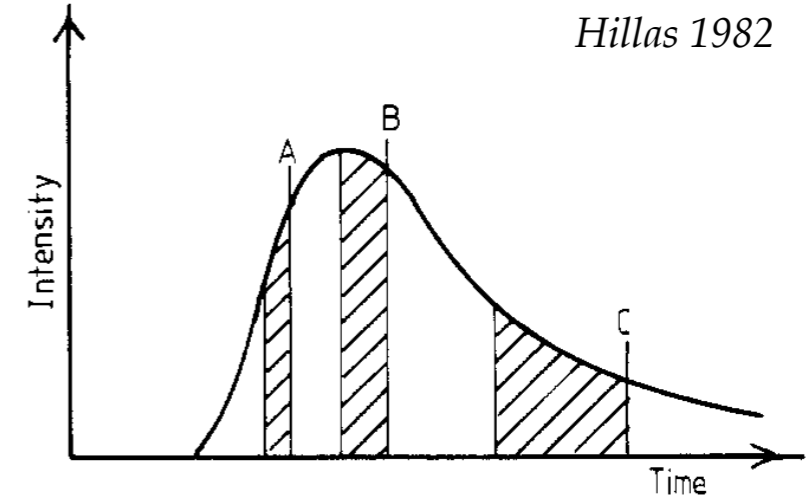


Fig. 4. The schematic view of a Cerenkov detector.



Hillas 1982

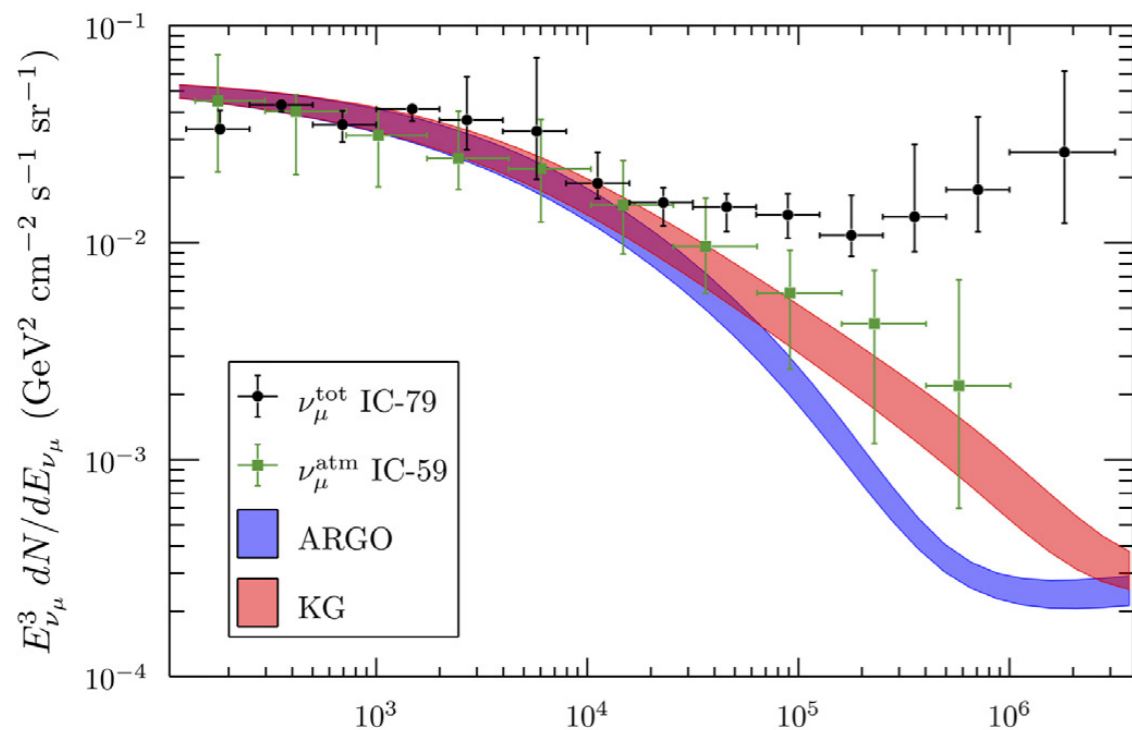
Portions of Cerenkov pulse received on the ground, each arriving from definite range of altitude

At 550 g/cm² this technique allows to measure the shower development well before the maximum, and to investigate the first few interactions

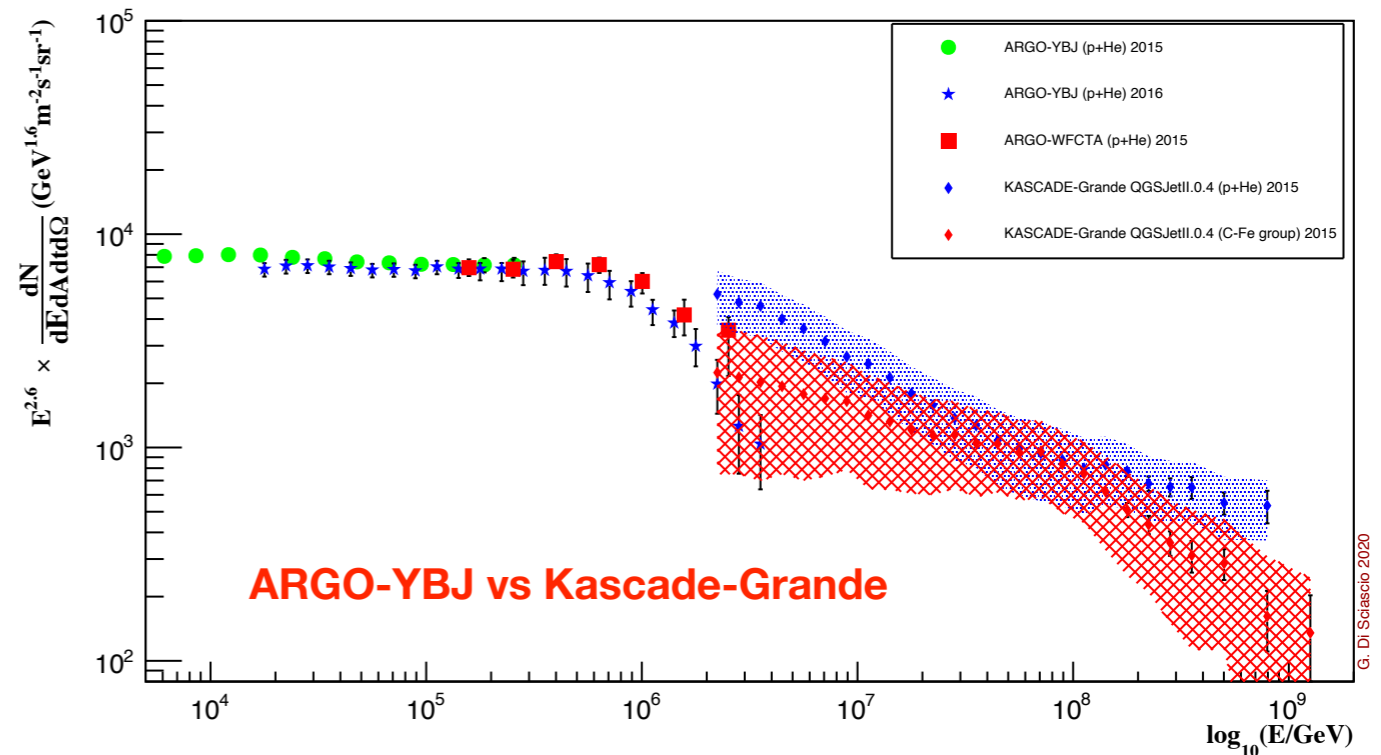
Knees and atmospheric neutrinos

The flux of atmospheric neutrinos is sensitive to the spectrum of parent cosmic rays.

“A clear distinction between an ARGO-like and a KASCADE-like knee seems possible at energies ≥ 100 TeV if the atmospheric neutrinos could be properly tagged.”



Mascaretti, Blasi, Evoli (2020) E_{ν_μ} (GeV)



“Unfortunately this is also the energy region where the total neutrino flux detected by IceCube departs from the existing predictions for atmospheric neutrinos. This is usually interpreted as the onset of a neutrino component having an astrophysical origin. So far, the sources of such neutrinos remain unknown.”

"Current experimental uncertainties do not allow to draw firm conclusions."